

# BERNSTEIN-BÉZIER BASES FOR TETRAHEDRAL FINITE ELEMENTS

MARK AINSWORTH AND GUOSHENG FU

ABSTRACT. We present a new set of basis functions for  $H(\text{curl})$ -conforming,  $H(\text{div})$ -conforming, and  $L^2$ -conforming finite elements of arbitrary order on a tetrahedron. The basis functions are expressed in terms of Bernstein polynomials and augment the natural  $H^1$ -conforming Bernstein basis. The basis functions respect the differential operators, namely, the gradients of the high-order  $H^1$ -conforming Bernstein-Bézier basis functions form part of the  $H(\text{curl})$ -conforming basis, and the curl of the high-order, non-gradients  $H(\text{curl})$ -conforming basis functions form part of the  $H(\text{div})$ -conforming basis, and the divergence of the high-order, non-curl  $H(\text{div})$ -conforming basis functions form part of the  $L^2$ -conforming basis.

Procedures are given for the efficient computation of the mass and stiffness matrices with these basis functions without using quadrature rules for (piecewise) constant coefficients on affine tetrahedra. Numerical results are presented to illustrate the use of the basis to approximate representative problems.

## 1. INTRODUCTION

Let  $\mathbb{P}_n$  be the space of polynomials of degree no greater than  $n$  on the tetrahedron,  $\tilde{\mathbb{P}}_n$  is the space of homogeneous polynomials of degree  $n$ , and  $\mathbb{P}_n^3 := [\mathbb{P}_n, \mathbb{P}_n, \mathbb{P}_n]^T$  is the vector space whose components lie in  $\mathbb{P}_n$ . We present a set of Bernstein-Bézier bases for the following two families of arbitrary order polynomial exact sequences on a tetrahedron  $T$ :

TABLE 1. Two exact sequences on a tetrahedron  $T$

	$H^1(T)$		$H(\text{curl}; T)$		$H(\text{div}; T)$		$L^2(T)$
First sequence:	$\mathbb{P}_{n+1}$	$\xrightarrow{\nabla}$	$\mathbb{P}_n^3 \oplus \mathbf{x} \times \tilde{\mathbb{P}}_n^3$	$\xrightarrow{\nabla \times}$	$\mathbb{P}_n^3 \oplus \mathbf{x} \tilde{\mathbb{P}}_n$	$\xrightarrow{\nabla \cdot}$	$\mathbb{P}_n$
Second sequence:	$\mathbb{P}_{n+2}$	$\xrightarrow{\nabla}$	$\mathbb{P}_{n+1}^3$	$\xrightarrow{\nabla \times}$	$\mathbb{P}_n^3$	$\xrightarrow{\nabla \cdot}$	$\mathbb{P}_{n-1}$

The basis for the  $H^1$ -case is taken to be the standard Bernstein polynomials as in [2]. The basis for the  $H(\text{curl})$ ,  $H(\text{div})$  and  $L^2$  cases are also constructed in terms of Bernstein polynomials in such a way that: the gradients of the high-order  $H^1$ -conforming Bernstein-Bézier basis functions are part of the  $H(\text{curl})$ -conforming basis; the curl of the high-order, non-gradient  $H(\text{curl})$ -conforming basis functions are part of the  $H(\text{div})$ -conforming basis; and, the divergence of the high-order, non-curl  $H(\text{div})$ -conforming basis functions are part of the  $L^2$ -conforming basis.

The construction of high-order finite element basis functions for the polynomial exact sequences has been extensively studied in the literature, see the hierarchical bases in [4, 6, 12], and the Bernstein-Bézier bases in [2, 3, 5]. Previous work [2]

---

1991 *Mathematics Subject Classification.* 65N30. 65Y20. 65D17. 68U07.

has demonstrated that using the Bernstein polynomials as basis functions for the  $H^1$ -case offers a number of advantages including enabling optimal complexity assembly of the stiffness and mass matrices even for nonlinear problems on non-affine triangulations. The current work shows that these, and other advantages of the Bernstein-Bézier basis are not confined to the  $H^1$ -case but extend to the whole de Rham sequence.

Quite apart from computational consideration, the Bernstein polynomials provide a convenient tool for theoretical work on splines [8] and were used in [5] to present alternative set of basis functions for the de Rham sequence. Comparing with the Bernstein-Bézier basis introduced in [5], our basis enjoys the so-called *local exact sequence* property [12], which means that the exact sequence property holds at the basis function level: gradients of the high-order  $H^1$ -conforming basis functions form part of the  $H(\text{curl})$ -conforming basis functions; curl of the high-order, non-gradient  $H(\text{curl})$ -conforming basis functions form part of the  $H(\text{div})$ -conforming basis functions; and, divergence of the high-order, non-curl  $H(\text{div})$ -conforming basis functions form part of the  $L^2$ -conforming basis functions. The clear separation of the gradients and non-gradients for the  $H(\text{curl})$ -conforming basis, and divergence-free functions and non-divergence-free functions for the  $H(\text{div})$ -conforming basis is not only satisfying from a theoretical standpoint, but can also be exploited in the practical application of the bases.

The rest of the paper is organized as follows: in Section 2, we present the main results of the basis functions for the two sequences in Table 1. In Section 3 and Section 4, we present details of the construction of the  $H(\text{curl})$ -conforming basis, and the  $H(\text{div})$ -conforming basis, respectively. Then, in Section 5, we discuss the efficient implementation of our basis for constant coefficient problems on affine tetrahedral elements. We conclude in Section 6 with numerical results validating our theoretical findings.

## 2. MAIN RESULTS

In this section, we summarize the main results concerning the Bernstein-Bézier basis functions for the  $H(\text{curl})$ - and  $H(\text{div})$ -conforming finite elements on a tetrahedron  $T := \text{conv}(\mathbf{x}_1, \mathbf{x}_2, \mathbf{x}_3, \mathbf{x}_4)$ . Combined with the Bernstein-Bézier basis for  $H^1$ -conforming finite elements [1], we thereby obtain a set of basis functions, which respect the differential operators, for the two polynomial de Rham sequences in Table 1, which corresponding to Nédélec spaces of the first and second kinds. We begin by collecting some useful notation with which to present the bases.

**2.1. Notation, index sets, and domain points.** Standard multi-index notations will be used throughout. In particular, for  $\boldsymbol{\alpha} \in \mathbb{Z}_+^{d+1}$ , we define  $|\boldsymbol{\alpha}| = \sum_{k=1}^{d+1} \alpha_k$ ,  $\boldsymbol{\alpha}! = \prod_{k=1}^{d+1} \alpha_k!$  and  $\binom{|\boldsymbol{\alpha}|}{\boldsymbol{\alpha}} = |\boldsymbol{\alpha}|! / \boldsymbol{\alpha}!$ . If  $\boldsymbol{\lambda} = (\lambda_1, \lambda_2, \dots, \lambda_{d+1}) \in \mathbb{R}^{d+1}$ , then we define  $\boldsymbol{\lambda}^{\boldsymbol{\alpha}} = \prod_{k=1}^d \lambda_k^{\alpha_k}$ . Given a pair  $\boldsymbol{\alpha}, \boldsymbol{\beta} \in \mathbb{Z}_+^{d+1}$ ,  $\boldsymbol{\alpha} \leq \boldsymbol{\beta}$  if and only if  $\alpha_k \leq \beta_k$ ,  $k = 1, \dots, d+1$  and, in this case,  $\binom{\boldsymbol{\beta}}{\boldsymbol{\alpha}} = \prod_{k=1}^{d+1} \binom{\beta_k}{\alpha_k}$ . An indexing set  $\mathcal{I}_d^n$  is defined by

$$\mathcal{I}_d^n = \{\boldsymbol{\alpha} \in \mathbb{Z}_+^{d+1} : |\boldsymbol{\alpha}| = n\}. \quad (1)$$

In this paper, we are mostly concerned with the three dimensional case  $d = 3$ . For  $d = 3$ , let  $\mathbf{e}_\ell \in \mathcal{I}_3^1$  ( $\ell = 1, 2, 3, 4$ ) denote the multi-index whose  $\ell$ -th entry is unity and whose remaining entries vanish.

Let  $T$  be a non-degenerate tetrahedron in  $\mathbb{R}^3$  given by  $\text{conv}(\mathbf{x}_1, \mathbf{x}_2, \mathbf{x}_3, \mathbf{x}_4)$ . The set  $\mathcal{D}_n(T) = \{\mathbf{x}_\alpha : \alpha \in \mathcal{I}_3^n\}$  consists of the *domain points* of the tetrahedron  $T$  defined by

$$\mathbf{x}_\alpha = \frac{1}{n} \sum_{k=1}^4 \alpha_k \mathbf{x}_k. \quad (2)$$

We denote the edge-based, face-based, and cell-based bubble index subsets of  $\mathcal{I}_3^n$  as follows: for an edge  $E = (\mathbf{x}_{e_1}, \mathbf{x}_{e_2}) \subset T$ ,

$$\mathring{\mathcal{I}}_3^n(E) = \{\alpha \in \mathcal{I}_3^n : \alpha_i > 0 \text{ if } i \in \{e_1, e_2\}, \alpha_i = 0 \text{ otherwise}\} \quad (3a)$$

for a face  $F = (\mathbf{x}_{f_1}, \mathbf{x}_{f_2}, \mathbf{x}_{f_3}) \subset T$ ,

$$\mathring{\mathcal{I}}_3^n(F) = \{\alpha \in \mathcal{I}_3^n : \alpha_i > 0 \text{ if } i \in \{f_1, f_2, f_3\}, \alpha_i = 0 \text{ otherwise}\} \quad (3b)$$

and for the element  $T$ ,

$$\mathring{\mathcal{I}}_3^n = \{\alpha \in \mathcal{I}_3^n : \alpha_i > 0 \text{ for all } i\}, \quad (3c)$$

The collection of these bubble index sets is denoted as

$$\begin{aligned} \tilde{\mathcal{I}}_3^n &:= \mathcal{I}_3^n - \{n\mathbf{e}_\ell : 1 \leq \ell \leq 4\} \\ &= \bigoplus_{E \in \mathcal{E}(T)} \mathring{\mathcal{I}}_3^n(E) \bigoplus_{F \in \mathcal{F}(T)} \mathring{\mathcal{I}}_3^n(F) \bigoplus \mathring{\mathcal{I}}_3^n. \end{aligned} \quad (3d)$$

where  $\mathcal{E}(T)$  and  $\mathcal{F}(T)$  are the collection of edges and faces, respectively, of the tetrahedron  $T$ .

We also denote the set of indices whose corresponding domain points lie on the face  $F = (\mathbf{x}_{f_1}, \mathbf{x}_{f_2}, \mathbf{x}_{f_3})$  as

$$\tilde{\mathcal{I}}_3^n(F) := \{\alpha \in \mathcal{I}_3^n : \alpha_i = 0, \quad i \notin \{f_1, f_2, f_3\}\}. \quad (3e)$$

Moreover, the index subsets of co-dimension 1 for  $\tilde{\mathcal{I}}_3^n(F)$  and  $\mathcal{I}_3^n$  will also be used:

$$\tilde{\mathcal{I}}_3^n(F)' := \tilde{\mathcal{I}}_3^n(F) - \{\text{a single, arbitrary index in } \tilde{\mathcal{I}}_3^n(F)\}, \quad (3f)$$

$$\mathcal{I}_3^{n'} := \mathcal{I}_3^n - \{\text{a single, arbitrary index in } \mathcal{I}_3^n\}. \quad (3g)$$

**2.2. Barycentric coordinates and Bernstein polynomials.** The *barycentric coordinates* of a point  $\mathbf{x} \in \mathbb{R}^3$  with respect to the tetrahedron  $T$  are given by  $\boldsymbol{\lambda} = (\lambda_1, \lambda_2, \lambda_3, \lambda_4)$  and satisfy

$$\mathbf{x} = \sum_{k=1}^4 \lambda_k \mathbf{x}_k; \quad 1 = \sum_{k=1}^4 \lambda_k. \quad (4)$$

The *Bernstein polynomials* of degree  $n \in \mathbb{Z}_+$  associated with  $T$  are defined by

$$B_\alpha^n(\mathbf{x}) = \binom{n}{\alpha} \boldsymbol{\lambda}^\alpha, \quad \alpha \in \mathcal{I}_3^n. \quad (5)$$

**2.3. Geometric decomposition of the finite element spaces and their basis functions.** We follow the popular convention whereby basis functions are identified with dots placed at appropriate domain points. Our main result is collected in the following theorem, whose proof is postponed to Section 3 and Section 4 where we study details of the  $H(\text{curl})$ -basis and  $H(\text{div})$ -basis, respectively.

**Theorem 1.** *Let  $\mathcal{E}(T)$  be the collection of edges of  $T$ , and  $E \in \mathcal{E}(T)$  be any edge. Let  $\mathcal{F}(T)$  be the collection of faces of  $T$ , and  $F \in \mathcal{F}(T)$  be any face. The sets of functions defined in Table 2 form a basis for the corresponding space for arbitrary polynomial order  $n$ .*

*Moreover, the following geometric decomposition holds for the finite element spaces in the two sequences in Table 1:*

$$\begin{aligned}
\mathbb{P}_n &= S_{low} \oplus_{E \in \mathcal{E}(T)} S_n^E \oplus_{F \in \mathcal{F}(T)} S_n^F \oplus S_n^T \\
\mathbb{P}_n^3 \oplus \mathbf{x} \times \tilde{\mathbb{P}}_n^3 &= \mathbf{E}_{low} \oplus_{E \in \mathcal{E}(T)} \nabla S_{n+1}^E \oplus_{F \in \mathcal{F}(T)} \left( \nabla S_{n+1}^F \oplus \mathbf{E}_n^F \right) \oplus \left( \nabla S_{n+1}^T \oplus \mathbf{E}_{n+1}^T \right) \\
\mathbb{P}_n^3 &= \mathbf{E}_{low} \oplus_{E \in \mathcal{E}(T)} \nabla S_{n+1}^E \oplus_{F \in \mathcal{F}(T)} \left( \nabla S_{n+1}^F \oplus \mathbf{E}_{n-1}^F \right) \oplus \left( \nabla S_{n+1}^T \oplus \mathbf{E}_n^T \right) \\
\mathbb{P}_n^3 \oplus \mathbf{x} \tilde{\mathbb{P}}_n &= \mathbf{V}_{low} \oplus_{F \in \mathcal{F}(T)} \nabla \times \mathbf{E}_n^F \oplus \left( \nabla \times \mathbf{E}_{n+1}^T \oplus \mathbf{V}_n^T \right) \\
\mathbb{P}_n^3 &= \mathbf{V}_{low} \oplus_{F \in \mathcal{F}(T)} \nabla \times \mathbf{E}_n^F \oplus \left( \nabla \times \mathbf{E}_{n+1}^T \oplus \mathbf{V}_{n-1}^T \right) \\
\mathbb{P}_n &= W_{low} \oplus \nabla \cdot \mathbf{V}_n^T
\end{aligned}$$

TABLE 2. Local spaces and their basis. Here  $\omega_{ij}$  is the lowest-order edge element given in (16) in Section 3,  $\chi_\ell$  is the lowest-order face element given in (22) in Section 4,  $\Phi_\alpha^{FT,n}$  is the  $\mathbf{H}(\text{curl})$ -face bubble given in (17) and  $\Psi_{\ell,\alpha}^{T,n}$  is the  $\mathbf{H}(\text{curl})$ -cell bubble given in (18) in Section 3, and  $\Upsilon_\alpha^n$  is the  $\mathbf{H}(\text{div})$ -bubble function given in (23) in Section 4.

Lowest-order elements	
$S_{low}$ : $\text{span}\{\lambda_i : 1 \leq i \leq 4\}$	$\mathbf{E}_{low}$ : $\text{span}\{\omega_{ij} : 1 \leq i < j \leq 4\}$
$\mathbf{V}_{low}$ : $\text{span}\{\chi_\ell : 1 \leq \ell \leq 4\}$	$W_{low}$ : $\text{span}\{1\}$
$H^1$ edge, face, cell bubbles and their gradients	
$S_n^E$ : $\text{span}\{B_\alpha^n : \alpha \in \tilde{\mathcal{I}}_3^n(E)\}$	$\nabla S_n^E$ : $\text{span}\{\nabla B_\alpha^n : \alpha \in \tilde{\mathcal{I}}_3^n(E)\}$
$S_n^F$ : $\text{span}\{B_\alpha^n : \alpha \in \tilde{\mathcal{I}}_3^n(F)\}$	$\nabla S_n^F$ : $\text{span}\{\nabla B_\alpha^n : \alpha \in \tilde{\mathcal{I}}_3^n(F)\}$
$S_n^T$ : $\text{span}\{B_\alpha^n : \alpha \in \tilde{\mathcal{I}}_3^n\}$	$\nabla S_n^T$ : $\text{span}\{\nabla B_\alpha^n : \alpha \in \tilde{\mathcal{I}}_3^n\}$
$\mathbf{H}(\text{curl})$ face, cell bubbles and their curls	
$\mathbf{E}_n^F$ : $\text{span}\{\Phi_\alpha^{FT,n} : \alpha \in \tilde{\mathcal{I}}_3^n(F)'\}$	$\nabla \times \mathbf{E}_n^F$ : $\text{span}\{\nabla \times \Phi_\alpha^{FT,n} : \alpha \in \tilde{\mathcal{I}}_3^n(F)'\}$
$\mathbf{E}_n^T$ : $\text{span} \oplus_{\ell=1}^2 \{\Psi_{\ell,\alpha}^{T,n} : \alpha \in \tilde{\mathcal{I}}_3^{n+1}\} \oplus \{\Psi_{3,\alpha}^{T,n} : \alpha \in \tilde{\mathcal{I}}_3^{n+1}, \alpha_3 = 1\}$	$\nabla \times \mathbf{E}_n^T$ : $\text{span} \oplus_{\ell=1}^2 \{\nabla \times \Psi_{\ell,\alpha}^{T,n} : \alpha \in \tilde{\mathcal{I}}_3^{n+1}\} \oplus \{\nabla \times \Psi_{3,\alpha}^{T,n} : \alpha \in \tilde{\mathcal{I}}_3^{n+1}, \alpha_3 = 1\}$
$\mathbf{H}(\text{div})$ cell bubbles and their divergences	
$\mathbf{V}_n^T$ : $\text{span}\{\Upsilon_\alpha^n : \alpha \in \tilde{\mathcal{I}}_3^{n'}\}$	$\nabla \cdot \mathbf{V}_n^T$ : $\text{span}\{\nabla \cdot \Upsilon_\alpha^n : \alpha \in \tilde{\mathcal{I}}_3^{n'}\}$

We illustrate the result in Theorem 1 for each sequence in Table 3 and indicate the dimension of the spaces for each case.

We also collect different types of basis functions and the corresponding dimension counts for the  $\mathbf{H}(\text{curl})$ -space  $\mathbb{P}_n^3 \oplus \mathbf{x} \times \tilde{\mathbb{P}}_n^3$  and the  $\mathbf{H}(\text{div})$ -space  $\mathbb{P}_n^3 \oplus \mathbf{x} \tilde{\mathbb{P}}_n$ , along with the domain points (for  $n = 3$ ) in Table 4 and Table 5, respectively. The index corresponding to the top white circle (for Type 3  $\mathbf{H}(\text{curl})$ -bases, and Type 2 and Type 4  $\mathbf{H}(\text{div})$ -bases) in the domain points plots indicates arbitrarily chosen

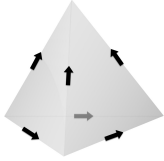
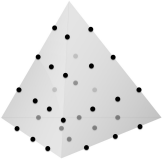
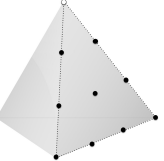
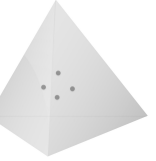
index used in the definition (3f)–(3g). Here for the Type 3  $\mathbf{H}(\text{curl})$ -face bubbles, we only plot the domain points for *one* face to make the plot more readable. Also, a domain point for Type 4  $\mathbf{H}(\text{curl})$ -cell bubbles corresponds to 2 basis functions  $(\Psi_{1,\alpha}^{n+1}, \Psi_{2,\alpha}^{n+1})$  if  $\alpha_3 > 1$ , and 3 basis functions  $(\Psi_{1,\alpha}^{n+1}, \Psi_{2,\alpha}^{n+1}, \Psi_{3,\alpha}^{n+1})$  if  $\alpha_3 = 1$ . The same information is presented for  $\mathbf{H}(\text{div})$ -bases.

In order to visualize the nature of the bases, we present contour plots of some representative basis functions in Figure 1 and Figure 2.

TABLE 3. Bernstein-Bézier basis for the two sequences in Table 1. Here  $\delta = 0$  for the first sequence and  $\delta = 1$  for the second sequence.

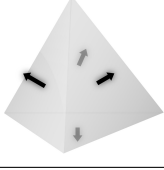
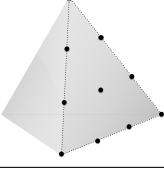
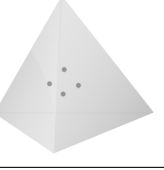
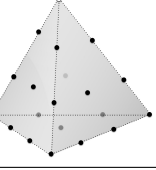
low	$S_{low}$	$\nabla \rightarrow$	$\mathbf{E}_{low}$	$\nabla \times \rightarrow$	$\mathbf{V}_{low}$	$\nabla \cdot \rightarrow$	$W_{low}$
Ndofs	4		6		4		1
edge	$S_{n+1+\delta}^E$	$\nabla \rightarrow$	$\nabla S_{n+1+\delta}^E$	$\nabla \times \rightarrow$	$\{0\}$		
Ndofs	$n + \delta$		$n + \delta$				
face	$S_{n+1+\delta}^F$	$\nabla \rightarrow$	$\nabla S_{n+1+\delta}^F \oplus \mathbf{E}_n^F$	$\nabla \times \rightarrow$	$\nabla \times \mathbf{E}_n^F$	$\nabla \cdot \rightarrow$	$\{0\}$
Ndofs	$\binom{n+\delta}{2}$		$\binom{n+\delta}{2} + \binom{n+2}{2} - 1$		$\binom{n+2}{2} - 1$		
cell	$S_{n+1+\delta}^T$	$\nabla \rightarrow$	$\nabla S_{n+1+\delta}^T \oplus \mathbf{E}_{n+1}^T$	$\nabla \times \rightarrow$	$\nabla \times \mathbf{E}_{n+1}^T \oplus \mathbf{V}_{n-\delta}^T$	$\nabla \cdot \rightarrow$	$\nabla \cdot \mathbf{V}_{n-\delta}^T$
Ndofs	$\binom{n+\delta}{3}$		$\binom{n+\delta}{3} + 2\binom{n+1}{3} + \binom{n}{2}$		$2\binom{n+1}{3} + \binom{n}{2} + \binom{n+3-\delta}{3} - 1$		$\binom{n+3-\delta}{3} - 1$

TABLE 4. Bases and domain points for the  $\mathbf{H}(\text{curl})$ -bases for the space  $\mathbb{P}_n^3 \oplus \mathbf{x} \times \widehat{\mathbb{P}}_n^3$

	Type 1 low	Type 2 gradients	Type 3 non-gradient face bubbles	Type 4 non-gradient cell bubbles
basis	$\chi_i$	$\nabla B_\alpha^n$	$\Phi_\alpha^{FT,n}$	$\Psi_{\ell,\alpha}^{n+1}$
Ndofs	6	$\binom{n+4}{3} - 4$	$4\binom{n+2}{2} - 4$	$2\binom{n+1}{3} + \binom{n}{2}$
domain points $n = 3$				

Although the basis are presented for the case where the local order is uniform. We may vary the polynomial degree associated to each edge, face and cell without compromising the local exact sequence property.

TABLE 5. Bases and domain points for the  $\mathbf{H}(\text{div})$ -bases for the space  $\mathbb{P}_n^3 \oplus \mathbf{x}\tilde{\mathbb{P}}_n$

	Type 1 low	Type 2 div-free face bubbles	Type 3 div-free cell bubbles	Type 4 non-curl cell bubbles
basis	$\chi_i$	$\nabla \times \Phi_{\alpha}^{FT,n}$	$\nabla \times \Psi_{\ell,\alpha}^{n+1}$	$\Upsilon_{\alpha}^n$
Ndofs	4	$4\binom{n+2}{2} - 4$	$2\binom{n+1}{3} + \binom{n}{2}$	$\binom{n+3}{3} - 1$
domain points $n = 3$				

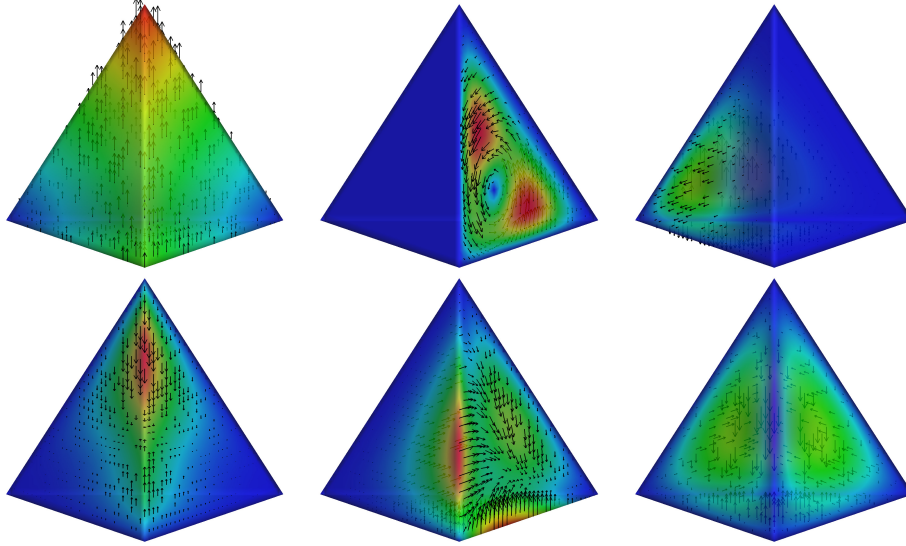


FIGURE 1. Top: left  $\omega_{24}$ , middle  $\Phi_{(0,2,1,1)}^{FT,4}$ , right:  $\Psi_{1,(2,1,1,1)}^{T,4}$ . Bottom: left  $\nabla B_{(0,2,0,2)}^4$ , middle  $\nabla B_{(0,2,1,1)}^4$ , right  $\nabla B_{(1,1,1,1)}^4$ .

**2.4. Embedded Sequences and Dimension Hierarchy.** Our basis also has the property that polynomial exact sequences on triangular elements which, in turn, contain exact sequences on edges, are “embedded” in our tetrahedral basis. These properties are illustrated in Figure 3, where the vertical arrows indicate the appropriate trace operator onto the lower dimensional entity.

We shall demonstrate explicitly show that the above *dimensional hierarchy* is satisfied at the level of basis functions for those listed in Theorem 1. This concept of dimensional hierarchy was introduced in [6, 12].

To this end, we introduce some further notation. Consider a triangular face  $F = \text{conv}\{\mathbf{x}_{i_1}, \mathbf{x}_{i_2}, \mathbf{x}_{i_3}\} \in \mathcal{F}(T)$  whose outward unit normal vector given as  $\mathbf{n}_F$ . We denote the set  $\mathbf{I}_F := \{i_1, i_2, i_3\}$  where  $i_1, i_2, i_3 \in \{1, 2, 3, 4\}$  are three distinct indices,

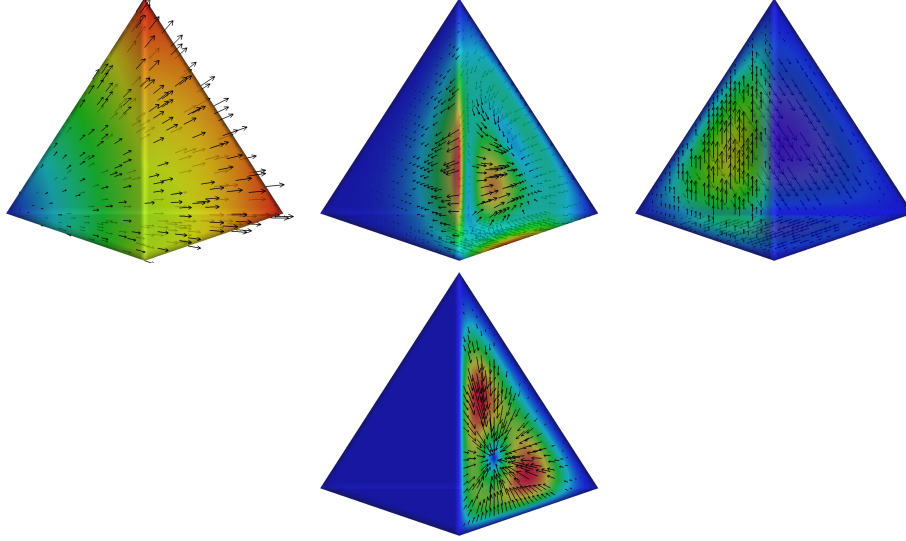


FIGURE 2. Top: left  $\chi_1$ , middle  $\nabla \times \Phi_{(0,2,1,1)}^{FT,4}$ , right:  $\nabla \times \Psi_{1,(2,1,1,1)}^{T,4}$ . Bottom:  $\Upsilon_{(0,2,1,1)}^4$ .

FIGURE 3. Embedded Sequence

First Sequence							
Tetrahedron:	$\mathbb{P}_{n+1}$	$\xrightarrow{\nabla}$	$\mathbb{P}_n^3 \oplus \mathbf{x} \times \tilde{\mathbb{P}}_n^3$	$\xrightarrow{\nabla \times}$	$\mathbb{P}_n^3 \oplus \mathbf{x} \tilde{\mathbb{P}}_n$	$\xrightarrow{\nabla \cdot}$	$\mathbb{P}_n$
	$\downarrow \text{tr}$		$\downarrow \text{tr}$		$\downarrow \text{tr}$		
Triangle:	$\mathbb{P}_{n+1}$	$\xrightarrow{\nabla}$	$\mathbb{P}_n^2 \oplus \mathbf{x} \times \tilde{\mathbb{P}}_n$	$\xrightarrow{\nabla \times}$	$\mathbb{P}_n$		
	$\downarrow \text{tr}$		$\downarrow \text{tr}$				
Segment:	$\mathbb{P}_{n+1}$	$\xrightarrow{\nabla}$	$\mathbb{P}_n$				
Second Sequence							
Tetrahedron:	$\mathbb{P}_{n+2}$	$\xrightarrow{\nabla}$	$\mathbb{P}_{n+1}^3$	$\xrightarrow{\nabla \times}$	$\mathbb{P}_n^3$	$\xrightarrow{\nabla \cdot}$	$\mathbb{P}_{n-1}$
	$\downarrow \text{tr}$		$\downarrow \text{tr}$		$\downarrow \text{tr}$		
Triangle:	$\mathbb{P}_{n+2}$	$\xrightarrow{\nabla}$	$\mathbb{P}_{n+1}^2$	$\xrightarrow{\nabla \times}$	$\mathbb{P}_n$		
	$\downarrow \text{tr}$		$\downarrow \text{tr}$				
Segment:	$\mathbb{P}_{n+2}$	$\xrightarrow{\nabla}$	$\mathbb{P}_{n+1}$ ,				

and let  $i_4$  be the index in  $\{1, 2, 3, 4\} \setminus I_F$ . For any multi-index  $\alpha = (\alpha_1, \alpha_2, \alpha_3, \alpha_4) \in \mathcal{I}_3^n$ , we denote  $\alpha_F = (\alpha_{i_1}, \alpha_{i_2}, \alpha_{i_3}) \in \mathcal{I}_2^n$  to be its restriction onto the face  $F$ . We denote the barycentric coordinates of a point  $\mathbf{x} \in F$  with respect to the triangle  $F$

as  $\boldsymbol{\lambda}^F = (\lambda_1^F, \lambda_2^F, \lambda_3^F)$  where

$$\boldsymbol{x} = \sum_{k=1}^3 \lambda_k^F \boldsymbol{x}_{i_k}; \quad 1 = \sum_{k=1}^3 \lambda_k^F, \quad (6)$$

and define the Bernstein polynomials of degree  $n \in \mathbb{Z}_+$  associated with  $F$  as

$$B_{\boldsymbol{\alpha}}^{F,n}(\boldsymbol{x}) = \binom{n}{\boldsymbol{\alpha}} \boldsymbol{\lambda}^F(\boldsymbol{x})^{\boldsymbol{\alpha}}, \quad \boldsymbol{\alpha} \in \mathcal{I}_2^n, \quad \boldsymbol{x} \in F. \quad (7)$$

The differential operator “ $\nabla$ ” acting on scalar function on  $F$  is understood to be the two-dimensional *surface gradient*, and “ $\nabla \times$ ” acting on a two-dimensional vectorial function on  $F$  is understood to be the scalar *surface curl*. In other words, if  $F$  lies in the  $x - y$  plane, with  $\boldsymbol{n}_F = (0, 0, 1)^T$  as the outward unit normal vector, then

$$\nabla \phi = \begin{pmatrix} \partial_x \phi \\ \partial_y \phi \end{pmatrix}, \quad \nabla \times \begin{pmatrix} \phi_1 \\ \phi_2 \end{pmatrix} = \partial_x \phi_2 - \partial_y \phi_1.$$

Denoting the sets

$$\mathcal{I}_2^{n'} := \mathcal{I}_2^n - \{\text{a single, arbitrary index in } \mathcal{I}_2^n\}, \quad (8a)$$

$$\tilde{\mathcal{I}}_2^n := \mathcal{I}_2^n - \{(n, 0, 0), (0, n, 0), (0, 0, n)\}, \quad (8b)$$

It is known [3, Theorem 3.6], that the following collection of functions forms a basis for  $\mathbb{P}_n(F)^2 \oplus \boldsymbol{x} \times \tilde{\mathbb{P}}_n(F)$ :

$$\{\boldsymbol{\omega}_{12}^F, \boldsymbol{\omega}_{13}^F, \boldsymbol{\omega}_{23}^F\} \cup \{\nabla B_{\boldsymbol{\alpha}}^{F,n+1} : \boldsymbol{\alpha} \in \tilde{\mathcal{I}}_2^{n+1}\} \cup \{\boldsymbol{\Phi}_{\boldsymbol{\alpha}}^{F,n} : \boldsymbol{\alpha} \in \mathcal{I}_2^{n'}\}, \quad (9)$$

where the *lowest-order edge elements*  $\boldsymbol{\omega}_{ij}^F$  and the *bubble functions*  $\boldsymbol{\Phi}_{\boldsymbol{\alpha}}^{F,n}$  are given by

$$\boldsymbol{\omega}_{ij}^F := \lambda_i^F \nabla \lambda_j^F - \lambda_j^F \nabla \lambda_i^F, \quad 1 \leq i < j \leq 3, \quad (10)$$

$$\boldsymbol{\Phi}_{\boldsymbol{\alpha}}^{F,n} := (n+1) B_{\boldsymbol{\alpha}}^{F,n} (\alpha_1 \boldsymbol{\omega}_{23}^F - \alpha_2 \boldsymbol{\omega}_{13}^F + \alpha_3 \boldsymbol{\omega}_{12}^F). \quad (11)$$

Equally well, the collection of functions

$$\{\boldsymbol{\omega}_{12}^F, \boldsymbol{\omega}_{13}^F, \boldsymbol{\omega}_{23}^F\} \cup \{\nabla B_{\boldsymbol{\alpha}}^{F,n+1} : \boldsymbol{\alpha} \in \tilde{\mathcal{I}}_2^{n+1}\} \cup \{\boldsymbol{\Phi}_{\boldsymbol{\alpha}}^{F,n-1} : \boldsymbol{\alpha} \in \mathcal{I}_2^{n-1'}\}, \quad (12)$$

form a basis for the space  $\mathbb{P}_n(F)^2$ .

We define the following trace operators,

$$\text{tr}_F(\phi) := \phi|_F \quad \forall \phi \in H^1(T), \quad (13)$$

$$\text{tr}_{t,F}(\phi_k \nabla \lambda_{i_k}) := \phi_k|_F \nabla \lambda_k^F \quad \forall \phi_k \in H^1(T), \quad \forall k \in \{1, 2, 3\}, \quad (14)$$

$$\text{tr}_{n,F}(\phi_k \nabla \lambda_{i_k}) := \phi_k|_F \nabla \lambda_{i_k} \cdot \boldsymbol{n}_F \quad \forall \phi_k \in H^1(T), \quad \forall k \in \{1, 2, 3\}. \quad (15)$$

It is easy to verify that

- $\text{tr}_F(\lambda_{i_k}) = \lambda_k^F$  for  $k \in \{1, 2, 3\}$ ,
- $\text{tr}_{t,F}(\boldsymbol{\omega}_{i_k i_\ell}) = \boldsymbol{\omega}_{k\ell}^F$  for  $k, \ell \in \{1, 2, 3\}$ ,
- $\text{tr}_{n,F}(\boldsymbol{\chi}_{i_4}) = \frac{1}{2 \text{area}(F)}$ ,

whilst, for  $\boldsymbol{\alpha} \in \tilde{\mathcal{I}}_3^n(F)$ , we obtain

- $\text{tr}_F(B_{\boldsymbol{\alpha}}^n) = B_{\boldsymbol{\alpha}_F}^{F,n}$ ,
- $\text{tr}_{t,F}(\nabla B_{\boldsymbol{\alpha}}^n) = \nabla B_{\boldsymbol{\alpha}_F}^{F,n}$ ,  $\text{tr}_{t,F}(\boldsymbol{\Phi}_{\boldsymbol{\alpha}}^{FT,n}) = \boldsymbol{\Phi}_{\boldsymbol{\alpha}_F}^{F,n}$ ,
- $\text{tr}_{n,F}(\nabla \times \boldsymbol{\Phi}_{\boldsymbol{\alpha}}^{FT,n}) = \nabla \times \boldsymbol{\Phi}_{\boldsymbol{\alpha}_F}^{F,n}$ .

We can formally state the claim concerning the dimension hierarchy from a tetrahedron to its triangular face.



**Theorem 2.** *The traces of the three dimensional bases given in Theorem 1 define bases for finite element spaces on triangles:*

$$\begin{aligned}\mathbb{P}_n(F) &= \text{tr}_F \left( \oplus_{k \in \mathbf{I}_F} \{\lambda_k\} \oplus_{E \in \mathcal{E}(F)} S_n^E \oplus S_n^F \right) \\ \mathbb{P}_n(F)^2 \oplus \mathbf{x} \times \tilde{\mathbb{P}}_n(F) &= \mathbf{tr}_{t,F} \left( \oplus_{k,\ell \in \mathbf{I}_F} \{\omega_{k\ell}\} \oplus_{E \in \mathcal{E}(F)} \nabla S_{n+1}^E \oplus \nabla S_{n+1}^F \oplus \mathbf{E}_n^F \right) \\ \mathbb{P}_n(F)^2 &= \mathbf{tr}_{t,F} \left( \oplus_{k,\ell \in \mathbf{I}_F} \{\omega_{k\ell}\} \oplus_{E \in \mathcal{E}(F)} \nabla S_{n+1}^E \oplus \nabla S_{n+1}^F \oplus \mathbf{E}_{n-1}^F \right) \\ \mathbb{P}_n(F) &= \text{tr}_{n,F} \left( \{\chi_{i_4}\} \oplus \nabla \times \mathbf{E}_n^F \right)\end{aligned}$$

Moreover, a similar dimension hierarchy holds for the restriction of basis functions on triangles to its edges.

**2.5. Vectorial function spaces.** To end this section, we collect notation for function spaces on the tetrahedral  $T$  that will be in the next two sections:

$$\begin{aligned}\mathbf{H}(\text{curl}; T) &:= \{\mathbf{v} \in L^2(T)^3 : \nabla \times \mathbf{v} \in L^2(T)^3\}, \\ \mathbf{H}_0(\text{curl}; T) &:= \{\mathbf{v} \in \mathbf{H}(\text{curl}; T) : \mathbf{tr}_{t,F} \mathbf{v} = \mathbf{0}, \forall F \in \mathcal{F}(T)\}, \\ \mathbf{H}(\text{div}; T) &:= \{\mathbf{v} \in L^2(T)^3 : \nabla \cdot \mathbf{v} \in L^2(T)\}, \\ \mathbf{H}_0(\text{div}; T) &:= \{\mathbf{v} \in \mathbf{H}(\text{div}; T) : \text{tr}_{n,F} \mathbf{v} = 0, \forall F \in \mathcal{F}(T)\}, \\ \mathbf{H}(\text{div}^0; T) &:= \{\mathbf{v} \in \mathbf{H}(\text{div}; T) : \nabla \cdot \mathbf{v} = 0\}, \\ \mathbf{H}_0(\text{div}^0; T) &:= \{\mathbf{v} \in \mathbf{H}_0(\text{div}; T) : \nabla \cdot \mathbf{v} = 0\}, \\ L_0^2(T) &:= \{v \in L^2(T) : \int_T v = 0\}.\end{aligned}$$

### 3. BERNSTEIN-BÉZIER $\mathbf{H}(\text{curl})$ FINITE ELEMENTS ON A TETRAHEDRON

Here we construct Bernstein-Bézier basis for both first- and second-kind Nédélec  $\mathbf{H}(\text{curl})$ -finite element on a tetrahedron  $T$ :  $\mathbb{P}_n^3 \oplus \mathbf{x} \times \tilde{\mathbb{P}}_n^3$  and  $\mathbb{P}_n^3$ .

Following [3, 12], we seek a basis that gives a clear separation between the *gradients* of the polynomial basis for the  $H^1$  space, and the non-gradients. In two dimensions, see (9) and (12), the non-gradients consist of 2D lowest-order edge elements, and  $\mathbf{H}(\text{curl})$  face bubbles. In three dimensions, the non-gradients will consist of 3D lowest-order edge elements, the natural 3D liftings of the 2D  $\mathbf{H}(\text{curl})$  face bubbles, and a set of  $\mathbf{H}(\text{curl})$  cell bubbles, as we see in the next.

**3.1. Lowest-order edge elements.** The following lowest-order edge elements are well-known:

$$\omega_{ij} := \lambda_i \nabla \lambda_j - \lambda_j \nabla \lambda_i, \quad i, j \in \{1, 2, 3, 4\}. \quad (16)$$

The set  $\{\omega_{ij} : 1 \leq i < j \leq 4\}$  form a basis for the space  $\mathbb{P}_0^3 \oplus \mathbf{x} \times \tilde{\mathbb{P}}_0^3$ .

**3.2. Non-gradient  $\mathbf{H}(\text{curl})$  face bubbles.** The non-gradient  $\mathbf{H}(\text{curl})$  face bubbles are obtained by simply lifting the 2D  $\mathbf{H}(\text{curl})$  face bubbles on the triangular boundary into the tetrahedron.

Let  $F = \text{conv}(\mathbf{x}_{i_1}, \mathbf{x}_{i_2}, \mathbf{x}_{i_3})$  be a face of the tetrahedron  $T$ , and let  $i_4$  be the index such that where  $(i_1, i_2, i_3, i_4)$  is a permutation of  $(1, 2, 3, 4)$ . For  $\alpha \in \tilde{\mathcal{I}}_3^n(F)$ , we define the function

$$\Phi_\alpha^{F,T,n} := (n+1)B_\alpha^n(\alpha_{i_1} \omega_{i_2 i_3} + \alpha_{i_2} \omega_{i_3 i_1} + \alpha_{i_3} \omega_{i_1 i_2}). \quad (17)$$

The following result characterizes above functions.

**Lemma 1.** *For any face  $F_\ell \in \mathcal{F}(T)$ , we have*

$$\mathbf{tr}_{t, F_\ell} \Phi_\alpha^{FT, n} = \begin{cases} \Phi_{\alpha_F}^{F_\ell, n} & \text{if } F_\ell = F, \\ 0 & \text{if } F_\ell \neq F, \end{cases} \quad \forall \alpha \in \tilde{\mathcal{I}}_3^n(F).$$

Moreover, the set  $\{\Phi_\alpha^{FT, n} : \alpha \in \tilde{\mathcal{I}}_3^n(F)'\}$  consists of  $\binom{n+2}{2} - 1$  linearly independent functions belonging to  $\mathbb{P}_n^3 \oplus \mathbf{x} \times \tilde{\mathbb{P}}_n^3$ .

*Proof.* Since  $\omega_{ij} \in \mathbb{P}_0^3 \oplus \mathbf{x} \times \tilde{\mathbb{P}}_0^3$ , we get  $\Phi_\alpha^{FT, n} \in \mathbb{P}_n^3 \oplus \mathbf{x} \times \tilde{\mathbb{P}}_n^3$ . The trace property follows from straightforward calculation comparing (11) and (17). The linear independence of functions is a direct consequence of the linear independence of their tangential traces on the face  $F$ .  $\square$

**3.3. Non-gradient  $\mathbf{H}(\text{curl})$  cell bubbles.** We use the following vector field, for  $\ell \in \{1, 2, 3, 4\}$ , to obtain the  $\mathbf{H}(\text{curl})$  cell bubbles:

$$\Psi_{\ell, \alpha}^n = (n+1)B_{\alpha - e_\ell}^n \nabla \lambda_\ell - \frac{\alpha_\ell}{n+1} \nabla B_\alpha^{n+1}, \quad \alpha \in \dot{\mathcal{I}}_3^{n+1}. \quad (18)$$

We have the following result concerning the above functions, whose proof is quite technical, and is postponed to the Appendix.

**Lemma 2.** *Let  $\Psi_{\ell, \alpha}^{n+1}$ ,  $\alpha \in \dot{\mathcal{I}}_3^{n+2}$ , denote the vector fields defined in (18). Then  $\Psi_{\ell, \alpha}^{n+1} \in \mathbf{H}_0(\text{curl}; T) \cap \mathbb{P}_n^3 \oplus \mathbf{x} \times \tilde{\mathbb{P}}_n^3$ . Moreover, the set*

$$\bigoplus_{\ell=1}^2 \left\{ \Psi_{\ell, \alpha}^{n+1} : \alpha \in \dot{\mathcal{I}}_3^{n+2} \right\} \bigoplus \left\{ \Psi_{3, \alpha}^{n+1} : \alpha \in \dot{\mathcal{I}}_3^{n+2}, \alpha_3 = 1 \right\} \quad (19)$$

consists of  $2\binom{n+1}{3} + \binom{n}{2}$  linearly independent vector fields in  $\mathbf{H}_0(\text{curl}; T) \cap \mathbb{P}_n^3 \oplus \mathbf{x} \times \tilde{\mathbb{P}}_n^3$ , whose curl set

$$\bigoplus_{\ell=1}^2 \left\{ \nabla \times \Psi_{\ell, \alpha}^{n+1} : \alpha \in \dot{\mathcal{I}}_3^{n+2} \right\} \bigoplus \left\{ \nabla \times \Psi_{3, \alpha}^{n+1} : \alpha \in \dot{\mathcal{I}}_3^{n+2}, \alpha_3 = 1 \right\} \quad (20)$$

form a basis for the divergence-free bubble space  $\mathbf{H}_0(\text{div}^0, T) \cap \mathbb{P}_n^3$ .

**3.4. Bernstein-Bézier  $\mathbf{H}(\text{curl})$  basis.** Combing the results in Lemma 1 and Lemma 2, and adding back the lowest-order edge elements along with the gradient fields, we obtain the Bernstein-Bézier  $\mathbf{H}(\text{curl})$  basis for both  $\mathbb{P}_n^3 \oplus \mathbf{x} \times \tilde{\mathbb{P}}_n^3$  ( $n \geq 0$ ), and  $\mathbb{P}_n^3$  ( $n \geq 1$ ) in the following theorem.

**Theorem 3.** *The set*

$$\begin{aligned} & \bigoplus \{ \omega_{ij} : 1 \leq i < j \leq 4 \} && \text{(lowest order)} \quad (21a) \\ & \bigoplus \{ \nabla B_\alpha^{n+1} : \alpha \in \dot{\mathcal{I}}_3^{n+1} \} && \text{(gradient fields)} \\ & \bigoplus_{F \in \mathcal{F}(T)} \{ \Phi_\alpha^{FT, n} : \alpha \in \tilde{\mathcal{I}}_3^n(F) \}' && \text{(face bubbles)} \\ & \bigoplus_{\ell=1}^2 \left\{ \Psi_{\ell, \alpha}^{n+1} : \alpha \in \dot{\mathcal{I}}_3^{n+2} \right\} \bigoplus \left\{ \Psi_{3, \alpha}^{n+1} : \alpha \in \dot{\mathcal{I}}_3^{n+2}, \alpha_3 = 1 \right\} && \text{(cell bubbles)} \end{aligned}$$

forms a basis for  $\mathbb{P}_n^3 \oplus \mathbf{x} \times \tilde{\mathbb{P}}_n^3$ , and the set

$$\begin{aligned} & \bigoplus \{\omega_{ij} : 1 \leq i < j \leq 4\} && \text{(lowest order)} \quad (21b) \\ & \bigoplus \{\nabla B_{\alpha}^{n+1} : \alpha \in \tilde{\mathcal{I}}_3^{n+1}\} && \text{(gradient fields)} \\ & \bigoplus_{F \in \mathcal{F}(T)} \{\Phi_{\alpha}^{FT, n-1} : \alpha \in \tilde{\mathcal{I}}_3^{n-1}(F)'\} && \text{(face bubbles)} \\ & \bigoplus_{\ell=1}^2 \{\Psi_{\ell, \alpha}^n : \alpha \in \tilde{\mathcal{I}}_3^{n+1}\} \bigoplus \{\Psi_{3, \alpha}^n : \alpha \in \tilde{\mathcal{I}}_3^{n+1}, \alpha_3 = 1\} && \text{(cell bubbles)} \end{aligned}$$

forms a basis for  $\mathbb{P}_n^3$ .

*Proof.* Let us focus on the proof of the first statement. The proof for the second is identical to that for the first, and is omitted.

By Lemma 1 and Lemma 2, we have functions contained in the respective sets in (21a) lie in  $\mathbb{P}_n^3 \oplus \mathbf{x} \times \tilde{\mathbb{P}}_n^3$ , whose dimensions are 6,  $\binom{n+4}{3} - 4$ ,  $4\binom{n+2}{2} - 4$ , and  $2\binom{n+1}{3} + \binom{n}{2}$ , leading to  $\frac{1}{2}(n+1)(n+3)(n+4) = \dim \mathbb{P}_n^3 \oplus \mathbf{x} \times \tilde{\mathbb{P}}_n^3$  functions in total.

We are left to show the linear independence of functions in these sets. Concerning the tangential trace on a face  $F_1 = \text{conv}\{\mathbf{x}_2, \mathbf{x}_{i_3}, \mathbf{x}_{i_4}\}$  of functions in each set, we have that only the following functions have non-vanishing traces:

$$\begin{aligned} & \bigoplus \{\omega_{k\ell} : k, \ell \in \{2, 3, 4\}\} && \text{(lowest order)} \\ & \bigoplus \{\nabla B_{\alpha}^{n+1} : \alpha \in \tilde{\mathcal{I}}_3^{n+1}, \alpha_1 = 0\} && \text{(gradient fields)} \\ & \bigoplus \{\Phi_{\alpha}^{F_4 T, n} : \alpha \in \tilde{\mathcal{I}}_3^n(F_4)'\} && \text{(face bubbles)}. \end{aligned}$$

The tangential traces of the above functions, in turn, form a set of basis for  $\mathbb{P}_n^3 \oplus \mathbf{x} \times \tilde{\mathbb{P}}_n^3$  on face  $F_4$ ; see Theorem 2. Hence, the above functions are themselves linearly independent. Working on the other faces, we obtain the linear independence of the functions in (21a) with non-vanishing tangential traces.

The remaining tangential-trace-free functions are the gradient bubbles

$$\{\nabla B_{\alpha}^{n+1} : \alpha \in \tilde{\mathcal{I}}_3^{n+1}\}$$

and the non-gradient bubbles in the set (19). The linear independence of these two sets is a direct consequence of Lemma 2. This completes the proof.  $\square$

#### 4. BERNSTEIN-BÉZIER $\mathbf{H}(\text{div})$ FINITE ELEMENT ON A TETRAHEDRON

Here we construct Bernstein-Bézier basis for both Raviart-Thomas (RT) and Brezzi-Douglas-Marini (BDM)  $\mathbf{H}(\text{div})$ -finite element on a tetrahedral  $T$ :  $\mathbb{P}_n^3 \oplus \mathbf{x} \times \tilde{\mathbb{P}}_n^3$  and  $\mathbb{P}_n^3$ .

Again, we seek a basis that gives a clear separation between the *curl* of the Bernstein polynomial basis for the  $\mathbf{H}(\text{curl})$  space constructed in the previous section, and the non-curl (not divergence-free)  $\mathbf{H}(\text{div})$  bubbles.

**4.1. Lowest-order face elements.** The following *lowest-order face elements* are well-known:

$$\chi_{\ell} := \lambda_i \nabla \lambda_j \times \nabla \lambda_k - \lambda_j \nabla \lambda_i \times \nabla \lambda_k + \lambda_k \nabla \lambda_i \times \nabla \lambda_j, \quad 1 \leq i < j < k \leq 4, \quad (22)$$

where  $(i, j, k, \ell)$  is a permutation of  $(1, 2, 3, 4)$ . The set  $\{\chi_{\ell} : 1 \leq \ell \leq 4\}$  form a basis of the space  $\mathbb{P}_0^3 \oplus \mathbf{x} \times \tilde{\mathbb{P}}_0^3$ .

**4.2. Non-curl  $\mathbf{H}(\text{div})$  bubbles.** The non-curl  $\mathbf{H}(\text{div})$  bubbles take a similar form as their two-dimensional companions in [3, Theorem 3.2]. We use the following vector field to obtain the  $\mathbf{H}(\text{div})$  bubbles:

$$\mathbf{Y}_\alpha^n = (n+1)B_\alpha^n \sum_{\ell=1}^4 (-1)^\ell \alpha_\ell \chi_\ell, \quad \alpha \in \mathcal{I}_3^n. \quad (23)$$

The following result characterizes the above functions, whose proof follows that for the two-dimensional case in [3, Lemma 3.1].

**Lemma 3.** *We have  $\mathbf{Y}_\alpha^n \in \mathbf{H}_0(\text{div}; T) \cap \mathbb{P}_n^3 \oplus \mathbf{x}\tilde{\mathbb{P}}_n$ . Moreover, the set*

$$\left\{ \mathbf{Y}_\alpha^n : \alpha \in \mathcal{I}_3^{n'} \right\} \quad (24)$$

*consists of  $\binom{n+3}{3} - 1$  linearly independent vector fields in  $\mathbf{H}_0(\text{div}; T) \cap \mathbb{P}_n^3 \oplus \mathbf{x}\tilde{\mathbb{P}}_n$ , whose divergence set*

$$\left\{ \nabla \cdot \mathbf{Y}_\alpha^n : \alpha \in \mathcal{I}_3^{n'} \right\} \quad (25)$$

*form a basis for the average-zero polynomial functions  $L_0^2(T) \cap \mathbb{P}_n$ .*

*Proof.* Since  $\chi_\ell \in \mathbb{P}_0^3 \oplus \mathbf{x}\tilde{\mathbb{P}}_0$  whose normal trace is constant on a single face and vanishes elsewhere, it is trivial to show  $\mathbf{Y}_\alpha^n \in \mathbf{H}_0(\text{div}; T) \cap \mathbb{P}_n^3 \oplus \mathbf{x}\tilde{\mathbb{P}}_n$  and  $\nabla \cdot \mathbf{Y}_\alpha^n \in L_0^2(T) \cap \mathbb{P}_n$ . Since the number of functions in either of the sets (24) and (25) is  $\#\mathcal{I}_3^{n'} = \binom{n+3}{3} - 1$ , which equals the dimension of the space  $L_0^2(T) \cap \mathbb{P}_n$ , we only need to prove the functions in the set (25) are linearly independent to conclude the proof of Lemma 3. We follow the proof of [3, Lemma 3.1].

Let coefficients  $c_\alpha$  be such that

$$\sum_{\alpha \in \mathcal{I}_3^n} c_\alpha \nabla \cdot \mathbf{Y}_\alpha^n = 0.$$

To simplify notation, we denote

$$\epsilon_{ijk} := \nabla \lambda_i \cdot (\nabla \lambda_j \times \nabla \lambda_k),$$

so that, in particular,

$$\epsilon_{123} = -\epsilon_{124} = \epsilon_{134} = -\epsilon_{234}.$$

Given a permutation  $(i, j, k, \ell)$  of  $(1, 2, 3, 4)$  with  $i < j < k$ , a simple calculation reveals that

$$\nabla \cdot (B_\alpha^n \lambda_i \nabla \lambda_j \times \nabla \lambda_k) = (\alpha_i + 1)(B_\alpha^n - B_{\alpha + \mathbf{e}_i - \mathbf{e}_\ell}^n) \epsilon_{ijk}. \quad (26)$$

By definition (23), we notice that  $\mathbf{Y}_\alpha^n$  consists of a linear combination of  $4 \times 3 = 12$  terms of the form  $B_\alpha^n \lambda_i \nabla \lambda_j \times \nabla \lambda_k$ . Applying (26), and after straightforward algebraic manipulation, we obtain that

$$\sum_{\alpha \in \mathcal{I}_3^n} c_\alpha \nabla \cdot \mathbf{Y}_\alpha^n = \epsilon_{123}(n+1) \sum_{\alpha \in \mathcal{I}_3^n} \tilde{c}_\alpha B_\alpha^n,$$

where

$$\tilde{c}_\alpha := \sum_{i=i}^4 \sum_{\substack{j=1 \\ j \neq i}}^4 \alpha_i (\alpha_j + 1) c_\alpha - \sum_{i=i}^4 \sum_{\substack{j=1 \\ j \neq i}}^4 (\alpha_i + 1) \alpha_j c_{\alpha + \mathbf{e}_i - \mathbf{e}_j}. \quad (27)$$

The linear independence of the Bernstein polynomials means that  $\tilde{c}_\alpha = 0$  for all  $\alpha \in \mathcal{I}_3^n$ . This latter condition constitutes a square linear system for the coefficients  $c_\alpha$ . The system is irreducible and weakly diagonally dominant, with the coefficients in each row of the system summing to zero. Hence, there exists  $c \in \mathbb{R}$  such that  $c_\alpha = c$  for all  $\alpha \in \mathcal{I}_3^n$ , which immediately implies the linear independence of functions in the set (25). This completes the proof.  $\square$

**4.3. Bernstein-Bézier  $\mathbf{H}(\text{div})$  basis.** Combing the results in Lemma 1, Lemma 2 and Lemma 3, we are ready to present the Bernstein-Bézier  $\mathbf{H}(\text{div})$  basis for both  $\mathbb{P}_n^3 \oplus \mathbf{x}\tilde{\mathbb{P}}_n(n \geq 0)$ , and  $\mathbb{P}_n^3(n \geq 1)$ . The results are collected in the following theorem.

**Theorem 4.** *The set*

$$\bigoplus_{\ell=1}^4 \{\chi_\ell\} \oplus \mathbf{W}^n \oplus \{\Upsilon_\alpha^n : \alpha \in \mathcal{I}_3^{n'}\} \quad (28a)$$

*forms a basis for  $\mathbb{P}_n^3 \oplus \mathbf{x}\tilde{\mathbb{P}}_n$ , and the set*

$$\bigoplus_{\ell=1}^4 \{\chi_\ell\} \oplus \mathbf{W}^n \oplus \{\Upsilon_\alpha^{n-1} : \alpha \in \mathcal{I}_3^{n-1'}\} \quad (28b)$$

*forms a basis for  $\mathbb{P}_n^3$ . Here the set  $\mathbf{W}^n$  contains the divergence-free fields obtained by taking the curl of the  $H(\text{curl})$ -basis functions:*

$$\begin{aligned} \mathbf{W}^n = & \bigoplus_{F \in \mathcal{F}(T)} \{\nabla \times \Phi_\alpha^{FT,n} : \alpha \in \tilde{\mathcal{I}}_3^n(F)'\} \\ & \bigoplus_{\ell=1}^2 \left\{ \nabla \times \Psi_{\ell,\alpha}^{n+1} : \alpha \in \tilde{\mathcal{I}}_3^{n+2} \right\} \oplus \left\{ \nabla \times \Psi_{3,\alpha}^{n+1} : \alpha \in \tilde{\mathcal{I}}_3^{n+2}, \alpha_3 = 1 \right\}. \end{aligned}$$

*Proof.* The fact that the functions in the sets lie in the finite element spaces and are linearly independent are due to Lemma 1, Lemma 2, and Lemma 3.

The number of functions contained in the respective sets in (28a) are 4,  $4 \binom{n+2}{2} - 4 + 2 \binom{n+1}{3} + \binom{n}{2}$ ,  $\binom{n+3}{3} - 1$ , leading to  $\frac{1}{2}(n+1)(n+2)(n+4) = \dim \mathbb{P}_n^3 \oplus \mathbf{x}\tilde{\mathbb{P}}_n$  functions in total; similarly, the total number of functions in (28b) is

$$\begin{aligned} 4 + 4 \binom{n+2}{2} - 4 + 2 \binom{n+1}{3} + \binom{n}{2} + \binom{n+2}{3} - 1 &= \frac{1}{2}(n+1)(n+2)(n+3) \\ &= \dim \mathbb{P}_n^3. \end{aligned}$$

Hence the sets (28a) and (28b) form bases for  $\mathbb{P}_n^3 \oplus \mathbf{x}\tilde{\mathbb{P}}_n$  and  $\mathbb{P}_n^3$ , respectively. This completes the proof.  $\square$

## 5. EFFICIENT COMPUTATION OF MASS AND STIFFNESS MATRICES WITH THE BASIS

In this section, we show how to explicitly compute the mass and stiffness matrices associated with the  $\mathbf{H}(\text{curl})$ - and  $\mathbf{H}(\text{div})$ -basis functions developed in the previous two sections for piecewise constant coefficients on an affine tetrahedron. Such explicit computation is made possible by the fact that our basis functions can be expressed as a linear combination of Bernstein polynomials, and then exploiting

the fact that the product of two Bernstein polynomials is another scaled Bernstein polynomial, and the integral of Bernstein polynomial has explicit formula.

**5.1. Notation.** The following geometric quantities of the tetrahedron  $T$  will be used:

$$\mathbf{t}_{ij} = \nabla \lambda_i \times \nabla \lambda_j, \quad (29a)$$

$$\epsilon_{ijk} = \mathbf{t}_{ij} \cdot \lambda_k, \quad (29b)$$

and

$$S_{i,j}^0 = \int_T \nabla \lambda_i \cdot \nabla \lambda_j \, dx, \quad (29c)$$

$$S_{ij,kl}^1 = \int_T \mathbf{t}_{ij} \cdot \mathbf{t}_{kl} \, dx, \quad (29d)$$

$$S_{ijk}^2 = \int_T (\epsilon_{ijk})^2 \, dx. \quad (29e)$$

We also use the Bernstein coefficients, which is independent of geometry:

$$M_{\alpha,\beta} = \frac{\binom{\alpha+\beta}{\alpha}}{\binom{|\alpha|+|\beta|}{|\alpha|} \binom{|\alpha|+|\beta|+3}{3}} \quad (30)$$

By properties of Bernstein polynomials, we have

$$B_{\alpha}^n B_{\beta}^m = \frac{\binom{\alpha+\beta}{\alpha}}{\binom{n+m}{n}} B_{\alpha+\beta}^{n+m}, \quad \int_T B_{\alpha}^n B_{\beta}^m \, dx = M_{\alpha,\beta} |T|.$$

**5.2. Transform to pure Bernstein-Bézier form.** First, let us transform all the basis functions along with their differential operators back to a linear combination of Bernstein polynomials.

**5.2.1.  $\mathbf{H}(\text{curl})$ -basis transformation.** We have four type of basis functions, namely, the lowest order edge elements  $\boldsymbol{\omega}_{ij}$  (Type 1), the gradient fields  $\nabla B_{\alpha}^{n+1}$  (Type 2), the face bubbles  $\boldsymbol{\Phi}_{\alpha}^{FT,n}$  (Type 3), and the cell bubbles  $\boldsymbol{\Psi}_{\ell,\alpha}^{T,n+1}$  (Type 4).

For compactness of the presentation, we just derive basis transformation for Type 3 basis below, and leave out details for the others. The transformation of these basis functions back to Bernstein-Bézier forms, along with their curls, are listed in Table 6, with the corresponding coefficients given in Table 7.

For Type 3 basis for the face  $F_{\ell} = \text{conv}\{\mathbf{x}_i, \mathbf{x}_j, \mathbf{x}_k\}$ , we have

$$\begin{aligned} \boldsymbol{\Phi}_{\alpha}^{F_{\ell}T,n} &= (n+1)B_{\alpha}^n(\alpha_i \boldsymbol{\omega}_{jk} - \alpha_j \boldsymbol{\omega}_{ik} + \alpha_k \boldsymbol{\omega}_{ij}) \\ &= (n+1)B_{\alpha}^n \left( \lambda_i(\alpha_k \nabla \lambda_j - \alpha_j \nabla \lambda_k) \right. \\ &\quad \left. + \lambda_j(\alpha_i \nabla \lambda_k - \alpha_k \nabla \lambda_i) \right. \\ &\quad \left. + \lambda_k(\alpha_j \nabla \lambda_i - \alpha_i \nabla \lambda_j) \right) \\ &= B_{\alpha+e_i}^{n+1}(\alpha_i+1)(\alpha_k \nabla \lambda_j - \alpha_j \nabla \lambda_k) \\ &\quad + B_{\alpha+e_j}^{n+1}(\alpha_j+1)(\alpha_i \nabla \lambda_k - \alpha_k \nabla \lambda_i) \\ &\quad + B_{\alpha+e_k}^{n+1}(\alpha_k+1)(\alpha_j \nabla \lambda_i - \alpha_i \nabla \lambda_j) \\ &= \sum_{\sigma \in \Sigma_{\ell}} B_{\alpha+e_{\sigma_1}}^{n+1}(\alpha_{\sigma_1}+1)(\alpha_{\sigma_3} \nabla \lambda_{\sigma_2} - \alpha_{\sigma_2} \nabla \lambda_{\sigma_3}) \end{aligned}$$

where  $\sigma = (\sigma_1, \sigma_2, \sigma_3)$  and the set

$$\Sigma_\ell := \{(i, j, k), (j, k, i), (k, i, j)\}, \quad (31)$$

where  $(i, j, k, \ell)$  form a permutation of  $(1, 2, 3, 4)$ . We also have

$$\begin{aligned} \nabla \times \Phi_\alpha^{F_\ell T, n} &= \sum_{\sigma \in \Sigma_\ell} (\alpha_{\sigma_1} + 1) \nabla B_{\alpha + e_{\sigma_1}}^{n+1} \times (\alpha_{\sigma_3} \nabla \lambda_{\sigma_2} - \alpha_{\sigma_2} \nabla \lambda_{\sigma_3}) \\ &= (n+1) \sum_{\sigma \in \Sigma_\ell} \sum_{k=1}^3 B_{\alpha + e_{\sigma_1} - e_{\sigma_k}}^n (\alpha_{\sigma_1} + 1) (\alpha_{\sigma_3} \mathbf{t}_{\sigma_k \sigma_2} - \alpha_{\sigma_2} \mathbf{t}_{\sigma_k \sigma_3}) \end{aligned}$$

TABLE 6. Bernstein-Bézier transformation of  $\mathbf{H}(\text{curl})$ -basis functions

	basis	BB-form	BB-form of its curl
Type 1	$\omega_{ij}$	$B_{e_i}^1 \nabla \lambda_j - B_{e_j}^1 \nabla \lambda_i$	$2 \mathbf{t}_{ij}$
Type 2	$\nabla B_\alpha^{n+1}$	$\sum_{i=1}^4 \mathbf{c}_{\alpha, i}^{(2)} B_{\alpha - e_i}^n$	$\mathbf{0}$
Type 3	$\Phi_\alpha^{F_\ell T, n}$	$\sum_{\sigma \in \Sigma_\ell} \mathbf{c}_{\alpha, \sigma}^{(3)} B_{\alpha + e_{\sigma_1}}^{n+1}$	$\sum_{\sigma \in \Sigma_\ell} \sum_{k=1}^3 \mathbf{d}_{\alpha, \sigma, k}^{(2)} B_{\alpha + e_{\sigma_1} - e_{\sigma_k}}^n$
Type 4	$\Psi_{\ell, \alpha}^{T, n+1}$	$\sum_{i=1}^4 \mathbf{c}_{\alpha, \ell, i}^{(4)} B_{\alpha - e_i}^{n+1}$	$\sum_{i=1}^4 \mathbf{d}_{\alpha, \ell, i}^{(3)} B_{\alpha - e_\ell - e_i}^n$

TABLE 7. Bernstein-Bézier transformation of  $\mathbf{H}(\text{curl})$ -basis functions

$\mathbf{c}_{\alpha, i}^{(2)} = (n+1) \nabla \lambda_i$
$\mathbf{c}_{\alpha, \sigma}^{(3)} = (\alpha_{\sigma_1} + 1) (\alpha_{\sigma_3} \nabla \lambda_{\sigma_2} - \alpha_{\sigma_2} \nabla \lambda_{\sigma_3})$
$\mathbf{d}_{\alpha, \sigma, k}^{(2)} = (n+1) (\alpha_{\sigma_1} + 1) (\alpha_{\sigma_3} \mathbf{t}_{\sigma_k \sigma_2} - \alpha_{\sigma_2} \mathbf{t}_{\sigma_k \sigma_3})$
$\mathbf{c}_{\alpha, \ell, i}^{(4)} = (\delta_{i\ell} (n+2) - \alpha_i) \nabla \lambda_i$
$\mathbf{d}_{\alpha, \ell, i}^{(3)} = (n+2)(n+1) \mathbf{t}_{i\ell}$

Here  $\delta_{i\ell}$  is the Kronecker delta.

5.2.2.  $\mathbf{H}(\text{div})$ -basis transformation. We also have four type of basis functions, namely, the lowest order face elements  $\chi_\ell$  (Type 1), the div-free face bubbles  $\nabla \times \Phi_\alpha^{F_\ell T, n}$  (Type 2), the div-free cell bubbles  $\nabla \times \Psi_{\ell, \alpha}^{T, n+1}$  (Type 3), and the non-curl cell bubbles  $\Upsilon_\alpha^n$  (Type 4). The transformation of these basis functions back to Bernstein-Bézier forms, along with their divergence, are listed in Table 8, where the coefficients  $\mathbf{d}_{\alpha, \sigma, k}^{(2)}$  and  $\mathbf{d}_{\alpha, \ell, i}^{(3)}$  are given in Table 7, and the coefficients  $\mathbf{d}_{\alpha, i}^{(4)}$  and  $\mathbf{g}_{\alpha, i, m}^{(2)}$  are given in Table 9. Again, we leave out details of the derivation. Here  $(i, j, k, \ell)$  form a cyclic permutation of  $(1, 2, 3, 4)$ .

5.3. Mass and stiffness matrices for  $\mathbf{H}(\text{curl})$  basis functions. Now, let us give formula for the mass and stiffness matrices for the  $\mathbf{H}(\text{curl})$  basis functions. For ease of notation, suppose that we have ordered the basis functions such that

$$\phi_p^1 = \omega_{i^p j^p}, \quad \phi_p^2 = \nabla B_{\alpha^p}^{n+1}, \quad \phi_p^3 = \Phi_{\alpha^p}^{F_{\ell^p} T, n}, \quad \phi_p^4 = \Psi_{\ell^p, \alpha^p}^{T, n+1}, \quad (32)$$

TABLE 8. Bernstein-Bézier transformation of  $\mathbf{H}(\text{div})$ -basis functions

	basis	BB-form	BB-form of its divergence
Type 1	$\chi_\ell$	$\sum_{\sigma \in \Sigma_{\ell p}} \mathbf{t}_{\sigma_2 \sigma_3} B_{e_{\sigma_1}}^1$	$(-1)^\ell 3 \epsilon_{123}$
Type 2	$\nabla \times \Phi_\alpha^{F_\ell T, n}$	$\sum_{\sigma \in \Sigma_\ell} \sum_{k=1}^4 \mathbf{d}_{\alpha, \sigma, k}^{(2)} B_{\alpha + e_{\sigma_1} - e_k}^n$	0
Type 3	$\nabla \times \Psi_{\ell, \alpha}^{T, n+1}$	$\sum_{i=1}^4 \mathbf{d}_{\alpha, \ell, i}^{(3)} B_{\alpha - e_\ell - e_i}^n$	0
Type 4	$\Upsilon_\alpha^n$	$\sum_{i=1}^4 \mathbf{d}_{\alpha, i}^{(4)} B_{\alpha + e_i}^{n+1}$	$\sum_{i=1}^4 \sum_{j=1}^4 g_{\alpha, i, j}^{(2)} B_{\alpha + e_i - e_j}^n$

TABLE 9. The coefficients

$$\begin{aligned} \mathbf{d}_{\alpha, i}^{(4)} &= (-1)^{i+1} (\alpha_i + 1) \sum_{\sigma \in \Sigma_i} \alpha_{\sigma_1} \mathbf{t}_{\sigma_2 \sigma_3} \\ g_{\alpha, i, j}^{(2)} &= (n+1)(\alpha_i + 1)(\delta_{ij} n - \alpha_j) \epsilon_{123} \end{aligned}$$

where  $p \in \mathbb{N}^+$  is an integer and the superscript  $p$  above indicates the corresponding indices are determined by  $p$ .

Due to the heterogeneity of the basis functions, the mass and stiffness matrices consists of  $4 \times 4$  blocks. By symmetry, we need to work out the computation for the 10 upper diagonal blocks for each matrix. Our calculation is given below.

5.3.1.  $\mathbf{H}(\text{curl})$  mass matrix. The first four blocks:

$$\begin{aligned} \int_T \phi_p^1 \cdot \phi_q^1 dx &= M_{\mathbf{e}_{ip}, \mathbf{e}_{iq}} S_{j^p, j^q}^0 - M_{\mathbf{e}_{ip}, \mathbf{e}_{jq}} S_{j^p, i^q}^0 \\ &\quad - M_{\mathbf{e}_{jp}, \mathbf{e}_{iq}} S_{i^p, j^q}^0 + M_{\mathbf{e}_{jp}, \mathbf{e}_{jq}} S_{i^p, i^q}^0 \end{aligned} \quad (33a)$$

$$\int_T \phi_p^1 \cdot \phi_q^2 dx = (n+1) \sum_{s=1}^4 (M_{\mathbf{e}_{ip}, \alpha^q - e_s} S_{j^p, s}^0 - M_{\mathbf{e}_{jp}, \alpha^q - e_s} S_{i^p, s}^0) \quad (33b)$$

$$\begin{aligned} \int_T \phi_p^1 \cdot \phi_q^3 dx &= \sum_{\sigma \in \Sigma_{\ell q}} M_{\mathbf{e}_{ip}, \alpha^q + e_{\sigma_1}} (\alpha_{\sigma_1}^q + 1) (\alpha_{\sigma_3}^q S_{j^p, \sigma_2}^0 - \alpha_{\sigma_2}^q S_{j^p, \sigma_3}^0) \\ &\quad - \sum_{\sigma \in \Sigma_{\ell q}} M_{\mathbf{e}_{jp}, \alpha^q + e_{\sigma_1}} (\alpha_{\sigma_1}^q + 1) (\alpha_{\sigma_3}^q S_{i^p, \sigma_2}^0 - \alpha_{\sigma_2}^q S_{i^p, \sigma_3}^0) \end{aligned} \quad (33c)$$

$$\int_T \phi_p^1 \cdot \phi_q^4 dx = \sum_{s=1}^4 (\delta_{s\ell q} (n+2) - \alpha_s^q) (M_{\mathbf{e}_{ip}, \alpha^q - e_s} S_{j^p, s}^0 - M_{\mathbf{e}_{jp}, \alpha^q - e_s} S_{i^p, s}^0) \quad (33d)$$



The next three blocks:

$$\int_T \phi_p^2 \cdot \phi_q^2 dx = (n+1)^2 \sum_{t=1}^4 \sum_{s=1}^4 M_{\alpha^p - e_t, \alpha^q - e_s} S_{t,s}^0 \quad (33e)$$

$$\int_T \phi_p^2 \cdot \phi_q^3 dx = (n+1) \sum_{t=1}^4 \sum_{\sigma \in \Sigma_{\ell^q}} M_{\alpha^p - e_t, \alpha^q + e_{\sigma_1}} (\alpha_{\sigma_1}^q + 1) (\alpha_{\sigma_3}^q S_{t,\sigma_2}^0 - \alpha_{\sigma_2}^q S_{t,\sigma_3}^0) \quad (33f)$$

$$\int_T \phi_p^2 \cdot \phi_q^4 dx = (n+1) \sum_{t=1}^4 \sum_{s=1}^4 (\delta_{s\ell^q} (n+2) - \alpha_s^q) M_{\alpha^p - e_t, \alpha^q - e_s} S_{t,s}^0 \quad (33g)$$

The next two blocks:

$$\int_T \phi_p^3 \cdot \phi_q^3 dx = \sum_{\tau \in \Sigma_{\ell^p}} \sum_{\sigma \in \Sigma_{\ell^q}} M_{\alpha^p + e_{\tau_1}, \alpha^q + e_{\sigma_1}} (\alpha_{\tau_1}^p + 1) (\alpha_{\sigma_1}^q + 1) (\alpha_{\tau_3}^p \alpha_{\sigma_3}^q S_{\tau_2, \sigma_2}^0 - \alpha_{\tau_3}^p \alpha_{\sigma_2}^q S_{\tau_2, \sigma_3}^0 - \alpha_{\tau_2}^p \alpha_{\sigma_3}^q S_{\tau_3, \sigma_2}^0 + \alpha_{\tau_2}^p \alpha_{\sigma_2}^q S_{\tau_3, \sigma_3}^0) \quad (33h)$$

$$\int_T \phi_p^3 \cdot \phi_q^4 dx = \sum_{\tau \in \Sigma_{\ell^p}} \sum_{s=1}^4 M_{\alpha^p + e_{\tau_1}, \alpha^q - e_s} (\delta_{s\ell^q} (n+2) - \alpha_s^q) (\alpha_{\sigma_1}^p + 1) (\alpha_{\tau_3}^p S_{\tau_2, s}^0 - \alpha_{\tau_2}^p S_{\tau_3, s}^0) \quad (33i)$$

The last block:

$$\int_T \phi_p^4 \cdot \phi_q^4 dx = \sum_{t=1}^4 \sum_{s=1}^4 M_{\alpha^q - e_t, \alpha^q - e_s} (\delta_{t\ell^p} (n+2) - \alpha_t^p) (\delta_{s\ell^q} (n+2) - \alpha_s^q) S_{t,s}^0 \quad (33j)$$

5.3.2.  **$\mathbf{H}$ (curl) stiffness matrix.** Since the curl of Type 2 basis (gradients) vanishes, we only need to calculate 6 blocks for the stiffness matrix. The first four blocks:

$$\int_T \nabla \times \phi_p^1 \cdot \nabla \times \phi_q^1 dx = 4 S_{i^p j^p, i^q j^q}^1 \quad (34a)$$

$$\int_T \nabla \times \phi_p^1 \cdot \nabla \times \phi_q^2 dx = 0 \quad (34b)$$

$$\int_T \nabla \times \phi_p^1 \cdot \nabla \times \phi_q^3 dx = \frac{12}{(n+2)(n+3)} \sum_{\sigma \in \Sigma_{\ell^q}} (\alpha_{\sigma_1}^q + 1) (\alpha_{\sigma_3}^q (S_{i^p j^p, \sigma_1 \sigma_2}^1 + S_{i^p j^p, \sigma_3 \sigma_2}^1) - \alpha_{\sigma_2}^q (S_{i^p j^p, \sigma_1 \sigma_3}^1 + S_{i^p j^p, \sigma_2 \sigma_3}^1)) \quad (34c)$$

$$\int_T \nabla \times \phi_p^1 \cdot \nabla \times \phi_q^4 dx = 0 \quad (34d)$$

The next three blocks are all zeros:

$$\int_T \nabla \times \phi_p^2 \cdot \nabla \times \phi_q^2 dx = 0$$

$$\int_T \nabla \times \phi_p^2 \cdot \nabla \times \phi_q^3 dx = 0$$

$$\int_T \nabla \times \phi_p^2 \cdot \nabla \times \phi_q^4 dx = 0$$

The next two blocks:

$$\begin{aligned} \int_T \nabla \times \phi_p^3 \cdot \nabla \times \phi_q^3 dx &= (n+1)^2 \sum_{\tau \in \Sigma_{\ell p}} \sum_{\ell=1}^3 \sum_{\sigma \in \Sigma_{\ell q}} \sum_{k=1}^3 M_{\alpha^p + e_{\tau_1} - e_{\tau_\ell}, \alpha^q + e_{\sigma_1} - e_{\sigma_k}} \\ &\quad (\alpha_{\tau_1}^p + 1)(\alpha_{\sigma_1}^q + 1)(\alpha_{\tau_3}^p \alpha_{\sigma_3}^q S_{\tau_\ell \tau_2, \sigma_k \sigma_2}^1 - \alpha_{\tau_3}^p \alpha_{\sigma_2}^q S_{\tau_\ell \tau_2, \sigma_k \sigma_3}^1 \\ &\quad - \alpha_{\tau_2}^p \alpha_{\sigma_3}^q S_{\tau_\ell \tau_3, \sigma_k \sigma_2}^1 + \alpha_{\tau_2}^p \alpha_{\sigma_2}^q S_{\tau_\ell \tau_3, \sigma_k \sigma_3}^1) \end{aligned} \quad (34e)$$

$$\begin{aligned} \int_T \nabla \times \phi_p^3 \cdot \nabla \times \phi_q^4 dx &= (n+2)(n+1)^2 \sum_{\tau \in \Sigma_{\ell p}} \sum_{\ell=1}^3 \sum_{i=1}^4 M_{\alpha^p + e_{\tau_1} - e_{\tau_\ell}, \alpha^q - e_{\ell^q} - e_i} \\ &\quad (\alpha_{\tau_1}^p + 1)(\alpha_{\tau_3}^p S_{\tau_\ell \tau_2, i \ell^q}^1 - \alpha_{\tau_2}^p S_{\tau_\ell \tau_3, i \ell^q}^1) \end{aligned} \quad (34f)$$

The last block:

$$\begin{aligned} \int_T \nabla \times \phi_p^4 \cdot \nabla \times \phi_q^4 dx &= \sum_{j=1}^4 \sum_{i=1}^4 (n+2)^2 (n+1)^2 \\ &\quad M_{\alpha^p - e_{\ell^p} - e_j, \alpha^q - e_{\ell^q} - e_i} S_{j \ell^p, i \ell^q}^1 \end{aligned} \quad (34g)$$

**5.4. Mass and stiffness matrices for  $\mathbf{H}(\text{div})$  basis functions.** Now, let us give formula for the mass and stiffness matrices for the  $\mathbf{H}(\text{div})$  basis functions. For ease of notation, suppose that we have ordered the basis functions such that

$$\psi_p^1 = \chi_{\ell^p}, \quad \psi_p^2 = \nabla \times \Phi_{\alpha^p}^{F_{\ell^p T}, n}, \quad \psi_p^3 = \nabla \times \Psi_{\ell^p, \alpha^p}^{T, n+1}, \quad \psi_p^4 = \Upsilon_{\alpha^p}^n, \quad (35)$$

where  $p \in \mathbb{N}^+$  is an integer and the superscript  $p$  above indicates the corresponding indices are determined by  $p$ .

Due to the heterogeneity of the basis functions, the mass and stiffness matrices consists of  $4 \times 4$  blocks. By symmetry, we need to work out the computation for the 10 upper diagonally blocks for each matrix. Our calculation is given below.

**5.4.1.  $\mathbf{H}(\text{div})$  mass matrix.** Since the Type 2 and Type 3  $\mathbf{H}(\text{div})$  basis is the curl of Type 3 and Type 4  $\mathbf{H}(\text{curl})$  basis, the corresponding matrix blocks is identical to the related stiffness matrix for  $\mathbf{H}(\text{curl})$  basis. Hence, we actually only need to compute  $10 - 3 = 7$  blocks this time.

The first four blocks:

$$\int_T \psi_p^1 \cdot \psi_q^1 dx = \sum_{\tau \in \Sigma_{\ell p}} \sum_{\sigma \in \Sigma_{\ell q}} M_{e_{\tau_1}, e_{\sigma_1}} S_{\tau_2 \tau_3, \sigma_2 \sigma_3}^1 \quad (36a)$$

$$\begin{aligned} \int_T \psi_p^1 \cdot \psi_q^2 dx &= (n+1) \sum_{\tau \in \Sigma_{\ell p}} \sum_{\sigma \in \Sigma_{\ell q}} \sum_{k=1}^3 M_{e_{\tau_1}, \alpha^q + e_{\sigma_1} - e_{\sigma_k}} \\ &\quad (\alpha_{\sigma_1}^q + 1)(\alpha_{\sigma_3}^q S_{\tau_2 \tau_3, \sigma_k \sigma_2}^1 - \alpha_{\sigma_2}^q S_{\tau_2 \tau_3, \sigma_k \sigma_3}^1) \end{aligned} \quad (36b)$$

$$\int_T \psi_p^1 \cdot \psi_q^3 dx = (n+2)(n+1) \sum_{\tau \in \Sigma_{\ell p}} \sum_{i=1}^4 M_{e_{\tau_1}, \alpha^q - e_{\ell^q} - e_i} S_{\tau_2 \tau_3, i \ell^q}^1 \quad (36c)$$

$$\int_T \psi_p^1 \cdot \psi_q^4 dx = \sum_{\tau \in \Sigma_{\ell p}} \sum_{i=1}^4 \sum_{\sigma \in \Sigma_i} (-1)^{i+1} (\alpha_i^q + 1) \alpha_{\sigma_1}^q M_{e_{\tau_1}, \alpha^q + e_i} S_{\tau_2 \tau_3, \sigma_2 \sigma_3}^1 \quad (36d)$$

The next three blocks:

$$\begin{aligned} \int_T \psi_p^2 \cdot \psi_q^2 dx &= (n+1)^2 \sum_{\tau \in \Sigma_{\ell^p}} \sum_{\ell=1}^3 \sum_{\sigma \in \Sigma_{\ell^q}} \sum_{k=1}^3 M_{\alpha^p + e_{\tau_1} - e_{\tau_\ell}, \alpha^q + e_{\sigma_1} - e_{\sigma_k}} \\ &\quad (\alpha_{\tau_1}^p + 1)(\alpha_{\sigma_1}^q + 1)(\alpha_{\tau_3}^p \alpha_{\sigma_3}^q S_{\tau_\ell \tau_2, \sigma_k \sigma_2}^1 - \alpha_{\tau_3}^p \alpha_{\sigma_2}^q S_{\tau_\ell \tau_2, \sigma_k \sigma_3}^1 \\ &\quad - \alpha_{\tau_2}^p \alpha_{\sigma_3}^q S_{\tau_\ell \tau_3, \sigma_k \sigma_2}^1 + \alpha_{\tau_2}^p \alpha_{\sigma_2}^q S_{\tau_\ell \tau_3, \sigma_k \sigma_3}^1) \end{aligned} \quad (36e)$$

$$\begin{aligned} \int_T \psi_p^2 \cdot \psi_q^3 dx &= (n+2)(n+1)^2 \sum_{\tau \in \Sigma_{\ell^p}} \sum_{\ell=1}^3 \sum_{i=1}^4 M_{\alpha^p + e_{\tau_1} - e_{\tau_\ell}, \alpha^q - e_{\ell^q} - e_i} \\ &\quad (\alpha_{\tau_1}^p + 1)(\alpha_{\tau_3}^p S_{\tau_\ell \tau_2, i \ell^q}^1 - \alpha_{\tau_2}^p S_{\tau_\ell \tau_3, i \ell^q}^1) \end{aligned} \quad (36f)$$

$$\begin{aligned} \int_T \psi_p^2 \cdot \psi_q^4 dx &= (n+1) \sum_{\tau \in \Sigma_{\ell^p}} \sum_{\ell=1}^3 \sum_{i=1}^4 \sum_{\sigma \in \Sigma_i} (-1)^{i+1} M_{\alpha^p + e_{\tau_1} - e_{\tau_\ell}, \alpha^q + e_i} \\ &\quad (\alpha_{\tau_1}^p + 1)(\alpha_i^q + 1) \alpha_{\sigma_1}^q (\alpha_{\tau_3}^p S_{\tau_\ell \tau_2, \sigma_2 \sigma_3}^1 - \alpha_{\tau_2}^p S_{\tau_\ell \tau_3, \sigma_2 \sigma_3}^1) \end{aligned} \quad (36g)$$

The next two blocks:

$$\begin{aligned} \int_T \psi_p^3 \cdot \psi_q^3 dx &= \sum_{j=1}^4 \sum_{i=1}^4 (n+2)^2 (n+1)^2 \\ &\quad M_{\alpha^p - e_{\ell^p} - e_j, \alpha^q - e_{\ell^q} - e_i} S_{j \ell^p, i \ell^q}^1 \end{aligned} \quad (36h)$$

$$\begin{aligned} \int_T \psi_p^3 \cdot \psi_q^4 dx &= (n+2)(n+1) \sum_{j=1}^4 \sum_{i=1}^4 \sum_{\sigma \in \Sigma_i} (-1)^{i+1} M_{\alpha^p - e_{\ell^p} - e_j, \alpha^q + e_i} \\ &\quad (\alpha_i^q + 1) \alpha_{\sigma_1}^q S_{j \ell^p, \sigma_2 \sigma_3}^1 \end{aligned} \quad (36i)$$

The last block:

$$\begin{aligned} \int_T \psi_p^4 \cdot \psi_q^4 dx &= \sum_{j=1}^4 \sum_{\tau \in \Sigma_j} \sum_{i=1}^4 \sum_{\sigma \in \Sigma_i} (-1)^{j+i} M_{\alpha^p + e_j, \alpha^q + e_i} \\ &\quad (\alpha_j^p + 1) \alpha_{\tau_1}^p (\alpha_i^q + 1) \alpha_{\sigma_1}^q S_{\tau_2 \tau_3, \sigma_2 \sigma_3}^1 \end{aligned} \quad (36j)$$

5.4.2.  **$\mathbf{H}(\text{div})$  stiffness matrix.** This time, we only need to compute three blocks since the divergence of Type 2 and Type 3 basis functions are zero.

$$\int_T \nabla \cdot \psi_p^1 \nabla \cdot \psi_q^1 dx = (-1)^{\ell^p + \ell^q} 9 S_{123}^2 \quad (37a)$$

$$\int_T \nabla \cdot \psi_p^1 \nabla \cdot \psi_q^4 dx = 0 \quad (37b)$$

$$\begin{aligned} \int_T \nabla \cdot \psi_p^4 \nabla \cdot \psi_q^4 dx &= (n+1)^2 \sum_{j=1}^4 \sum_{\ell=1}^4 \sum_{i=1}^4 \sum_{k=1}^4 (-1)^{i+j} M_{\alpha^p + e_j - e_\ell, \alpha^q + e_i - e_k} \\ &\quad (\alpha_j^p + 1)(\delta_{j\ell} n - \alpha_\ell)(\alpha_i^q + 1)(\delta_{ik} n - \alpha_k) S_{123}^2 \end{aligned} \quad (37c)$$

## 6. NUMERICAL EXAMPLES

We conclude with three examples which illustrate the use of the bases. We consider the case of constant data and affine tetrahedral elements although the ideas presented in [2] could be used to treat much more general scenarios. The stiffness and mass matrices are explicitly computed using the formula in Section

5 (along with proper ordering of degrees of freedom); while the integrals involving source terms are obtained via Stroud conical quadrature rules [2].

The first two examples were taken from [7] where, for the first time,  $\mathbf{H}(\text{curl})$  and  $\mathbf{H}(\text{div})$  Bernstein basis in [5] were implemented. The third example solve a mixed elliptic problem with a divergence-free vector solution, where we exploit the fact that our basis provides a clear separation of the divergence free functions to solve the problem with a reduced  $\mathbf{H}(\text{div})$  basis whereby all the Type 4 (not divergence-free)  $\mathbf{H}(\text{div})$  bubbles are omitted, coupled with a piecewise constant scalar field. The reduced basis approach produce exactly the same vector field approximation but requires fewer degrees of freedom (see e.g. [9, 10] on the use of reduced basis for incompressible flow problems).

**6.1. Maxwell eigenvalue problem.** We consider the problem of finding resonances  $\omega \in \mathbb{R}$  and eigenfunctions  $\mathbf{E} \in \mathbf{H}_0(\text{curl})$  such that

$$(\nabla \times \mathbf{E}, \nabla \times \mathbf{F})_{\Omega} = \omega^2 (\mathbf{E}, \mathbf{F})_{\Omega}, \quad \forall \mathbf{F} \in \mathbf{H}_0(\text{curl}).$$

Same as in [7], we consider the cube  $\Omega = [0, \pi]^3$  divided into 6 tetrahedra and study  $p$ -convergence of the finite element eigenvalue problem with Nédélec's  $\mathbf{H}(\text{curl})$  finite elements of first kind,  $\mathbb{P}_n^3 \oplus \mathbf{x} \times \tilde{\mathbb{P}}_n^3$ , using basis functions in Table 3. For this problem, the first eigenvalues are 2 with multiplicity 3, 3 with multiplicity 2, and 5 with multiplicity 6. We take the first 11 nonzero computed eigenvalues and measure the average error in each one in Figure 4. Similar convergence behavior as that in [7, Fig. 4.8] is obtained; in particular, we see that ten-digit accuracy in all three of the first eigenvalues is obtained when we reach degree 12, we also see round-off effect when degree is 13.

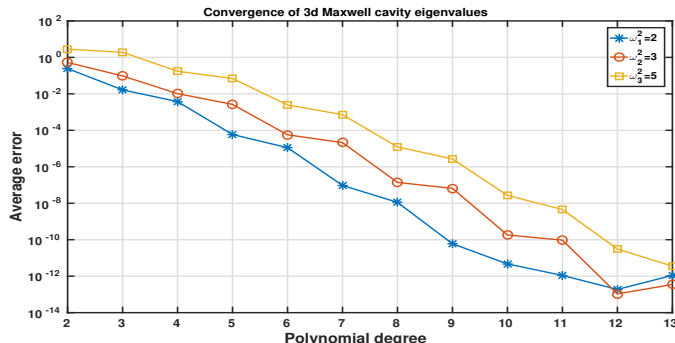


FIGURE 4. Error in the first three non-zero distinct eigenvalues for the three-dimensional cavity resonator problem

**6.2. Mixed Poisson problem.** Here we consider the mixed Poisson problem

$$\begin{aligned} \mathbf{u} + \nabla p &= 0 \\ \nabla \cdot \mathbf{u} &= f \end{aligned}$$

on a unit cube which homogeneous Dirichlet boundary conditions. We pick  $f$  such that the true solution is  $p(x, y, z) = \sin(\pi x) \sin(\pi y) \sin(\pi z)$ . Again, we divided the

unit cube into 6 tetrahedra and study  $p$ -convergence of the mixed finite elements: find  $(\mathbf{u}_h, p_h) \in \mathbf{V}_h \times W_h$  such that

$$\begin{aligned} (\mathbf{u}_h, \mathbf{v}_h)_\Omega - (p_h, \nabla \cdot \mathbf{v}_h)_\Omega &= 0 \\ (\nabla \cdot \mathbf{u}_h, q_h)_\Omega &= (f, q_h)_\Omega \end{aligned}$$

the stable finite element pair  $\mathbb{P}_n^3 \oplus \tilde{\mathbf{x}}\mathbb{P}_n \times \mathbb{P}_n$  using the basis functions in Table 3 is used in the computation. We use static condensation to condense out the interior degrees of freedom for the velocity and *average-zero* degrees of freedom for the potential, the resulting condensed system matrix consists of face degrees of freedom for velocity and piecewise constants for pressure. The size of the condensed system matrix, along with that of the original one, for various polynomial degree is listed in Table 10. We observe significant computational saving in terms of the global system matrix size by the static condensation. We remark that such static condensation relies on the fact that there are no inter-element communication for the internal degrees of freedom for velocity and average-zero degrees of freedom for the potential, hence they can be static condensed out using the face degrees of freedom for velocity and constant degree of freedom for potential in each element. If the potential degrees of freedom were not to have the constant and average-zero separation, as the basis used in [7], one might not be able to condense out any of the pressure degrees of freedom.

TABLE 10. Size of condensed system matrix  $K_c$  and original system matrix  $K_o$  for mixed Poisson problem on a six-tetrahedron mesh for polynomial degree 0 to 14

degree	0	1	2	3	4	5	6	7
size $K_c$	24	60	114	186	276	384	510	654
size $K_o$	24	96	240	480	840	1344	2016	2880
degree	8	9	10	11	12	13	14	
size $K_c$	816	996	1194	1410	1644	1896	2166	
size $K_o$	3960	5280	6864	8736	10920	13440	16320	

The  $L^2$ -error for the potential and velocity fields are plotted in Figure 5. We observe exponential convergence as expected. We also see similar jagged convergence in potential, with small drops from even up to odd degree followed by large drops from odd up to even degree, as documented in [7]. However, such jagged convergence behavior seems do not appear for the velocity approximation.

**6.3. Modified mixed Poisson problem.** Here we consider the following modified mixed Poisson problem

$$\begin{aligned} \mathbf{u} + \nabla p &= \mathbf{f} \\ \nabla \cdot \mathbf{u} &= 0 \end{aligned}$$

on a unit cube with homogeneous Dirichlet boundary conditions for scalar field  $p$ . We pick  $\mathbf{f}$  such that the true solution is  $p(x, y, z) = \sin(\pi x) \sin(\pi y) \sin(\pi z)$  and  $\mathbf{u}(x, y, z) = (0, \sin(\pi x) \cos(\pi y) \sin(\pi z), -\sin(\pi x) \sin(\pi y) \cos(\pi z))^T$ .

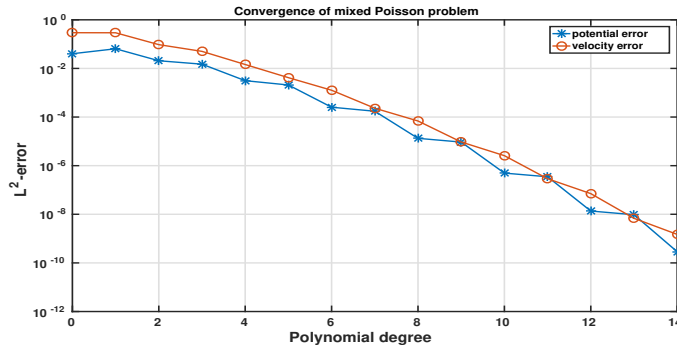


FIGURE 5. Convergence of the mixed finite element method as a function of the polynomial degree on a mesh with six tetrahedra.

This time, we study  $h$ -convergence of the mixed finite elements: find  $(\mathbf{u}_h, p_h) \in \mathbf{V}_h \times W_h$  such that

$$\begin{aligned} (\mathbf{u}_h, \mathbf{v}_h)_\Omega - (p_h, \nabla \cdot \mathbf{v}_h)_\Omega &= (\mathbf{f}, \mathbf{v}_h)_\Omega \\ (\nabla \cdot \mathbf{u}_h, q_h)_\Omega &= 0. \end{aligned}$$

In Figure 6, we plot  $L^2$ -error for the vector field for two finite element methods for polynomial degree 1, 3, 5 on five consecutive meshes obtained by cutting the unit cube to  $m^3$  congruent cubes and dividing each cube into 6 tetrahedra, we vary the (inverse) mesh size  $m$  from 2 to 10. The first method, labeled as Div-Free:NO in Figure 6, uses the Raviart-Thomas finite elements used in the previous test:

$$\mathbb{P}_n^3 \oplus \mathbf{x}\tilde{\mathbb{P}}_n \times \mathbb{P}_n = \left( \mathbf{V}_{low} \oplus_{F \in \mathcal{F}(K)} \nabla \times \mathbf{E}_n^F \oplus \nabla \times \mathbf{E}_{n+1}^T \oplus \mathbf{V}_n^T \right) \times \left( W_{low} \oplus \nabla \cdot \mathbf{V}_n^T \right),$$

the second method, labeled as Div-Free:YES in Figure 6, uses the following reduced (divergence-free) finite elements:

$$\left( \mathbf{V}_{low} \oplus_{F \in \mathcal{F}(K)} \nabla \times \mathbf{E}_n^F \oplus \nabla \times \mathbf{E}_{n+1}^T \right) \times W_{low}.$$

See definition of the above spaces in Section 2. It is easy to show that both methods produce the same vector approximation, which is clearly observed in Figure 6, where the optimal  $L^2$ -convergence error for the vector field for both methods are on top of each other. We list the global (static-condensed) number of degrees of freedom along with the local number of degrees of freedom for both methods in Table 11. While both methods share the same number of global degrees of freedom, the reduced basis approach has significant amount of local degrees of freedom reduction.

#### APPENDIX: PROOF OF LEMMA 2

*Proof.* Firstly, we show that  $\Psi_{\ell, \alpha}^{n+1}$  has vanishing tangential components on  $\partial T$  for  $\alpha \in \mathring{I}_{n+2}(T)$ . The vector field  $B_{\alpha - \mathbf{e}_\ell}^{n+1} \nabla \lambda_\ell$  has vanishing tangential components on the face  $F_\ell$  since  $\nabla \lambda_\ell$  points in the direction of the normal on face  $F_\ell$ , whilst the Bernstein polynomial  $B_{\alpha - \mathbf{e}_\ell}^{n+1}$  vanishes on the remaining faces since  $\alpha \in \mathring{I}_{n+2}(T)$ . Likewise, the Bernstein polynomial  $B_\alpha^{n+2}$  belongs to  $H_0^1(T)$  and so  $\nabla B_\alpha^{n+2} \in \mathbf{H}_0(\text{curl}; T)$ . Hence,  $\Psi_{\ell, \alpha}^{n+1} \in \mathbf{H}_0(\text{curl}; T)$ .

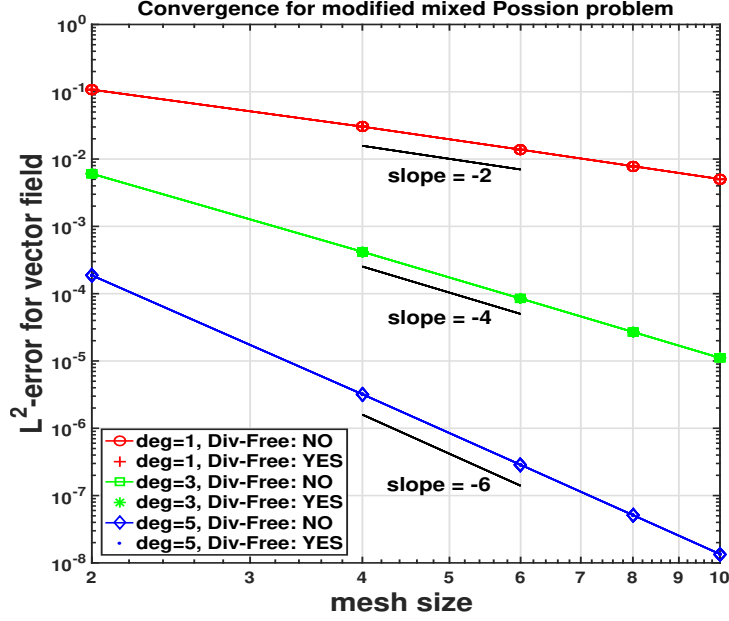


FIGURE 6.  $L^2$ -error for vector field of the modified mixed Poisson problem. Div-Free:NO is referred as the first (original) method, and Div-Free:YES is referred as the second (reduced) method.

TABLE 11. Number of degrees of freedom for the two methods.  $N_g$ : global number of dofs for both methods,  $N_l^{red}$ : local number of dofs for second method (with reduced basis),  $N_l$ : local number of dofs for first method.

Nelems	deg=1			deg=2			deg=3		
	$N_g$	$N_l^{red}$	$N_l$	$N_g$	$N_l^{red}$	$N_l$	$N_g$	$N_l^{red}$	$N_l$
48	408	0	288	1248	528	2352	2568	2400	7680
384	2976	0	2304	9024	4224	18816	18528	19200	61440
1296	9720	0	7776	29376	14256	63504	60264	64800	207360
3072	22656	0	18432	68352	33792	150528	140160	153600	491520
6000	43800	0	36000	132000	66000	294000	270600	300000	960000

Concerning membership of the Nédélec space  $\mathbb{P}_n^3 \oplus \mathbf{x} \times \widetilde{\mathbb{P}}_n^3$ , we begin with the observation that  $\Psi_{\ell, \alpha}^{n+1} \in \mathbb{P}_{n+1}^3$ . Consequently, in view of [11, Proposition 1], it suffices to show that  $\mathbf{x} \cdot \Psi_{\ell, \alpha}^{n+1} \in \mathbb{P}_{n+1}$ , where  $\mathbf{x} \in \mathbb{R}^3$  denotes the usual position vector of points in  $\mathbb{R}^3$ . Next, since the barycentric coordinates are affine functions of  $\mathbf{x}$ ,

$$(\mathbf{x} - \mathbf{x}_\ell) \cdot \nabla \lambda_m = \lambda_m(\mathbf{x}) - \lambda_m(\mathbf{x}_\ell) = \lambda_m(\mathbf{x}) - \delta_{\ell m}.$$

Hence,

$$(\mathbf{x} - \mathbf{x}_\ell) \cdot B_{\alpha - e_\ell}^{n+1} \nabla \lambda_\ell = (\lambda_\ell - 1) B_{\alpha - e_\ell}^{n+1} = \frac{\alpha_\ell}{n+2} B_{\alpha}^{n+2} - B_{\alpha - e_\ell}^{n+1},$$

thanks to the following elementary property of Bernstein polynomials

$$\lambda_m B_{\alpha - e_m}^{n-1} = \frac{\alpha_m}{n+2} B_{\alpha}^{n+2}.$$

The same property, along with identity  $\nabla B_{\alpha}^{n+1} = (n+1) \sum_{k=1}^4 B_{\alpha-e_k}^n \nabla \lambda_k$ , also gives

$$\begin{aligned} \frac{1}{n+2} (\mathbf{x} - \mathbf{x}_{\ell}) \cdot \nabla B_{\alpha}^{n+2} &= \sum_{m=1}^4 B_{\alpha-e_m}^{n+1} (\mathbf{x} - \mathbf{x}_{\ell}) \cdot \nabla \lambda_m \\ &= \sum_{m=1}^4 \lambda_m B_{\alpha-e_m}^{n+1} - B_{\alpha-e_{\ell}}^{n+1} \\ &= B_{\alpha}^{n+2} - B_{\alpha-e_{\ell}}^{n+1}, \end{aligned}$$

on recalling  $\sum_{m=1}^4 \alpha_m = n+2$ . Therefore,

$$(\mathbf{x} - \mathbf{x}_{\ell}) \cdot \Psi_{\ell, \alpha}^{n+1} = -(n+2 - \alpha_{\ell}) B_{\alpha-e_{\ell}}^{n+1},$$

or, equally well,  $\mathbf{x} \cdot \Psi_{\ell, \alpha}^{n+1} \in \mathbb{P}_{n+1}$ .

A simple calculation implies that the total number of functions in the sets in (19) is  $2\binom{n+1}{3} + \binom{n}{2}$ , which is equal to the dimension of divergence-free bubble space on a tetrahedral  $\mathbf{H}_0(\operatorname{div}^0; T) \cap \mathbb{P}_n^3$ . By exact sequence property, the fact that  $\Psi_{\ell, \alpha}^{n+1} \in \mathbb{P}_n^3 \oplus \mathbf{x} \times \tilde{\mathbb{P}}_n^3$  implies that  $\nabla \times \Psi_{\ell, \alpha}^{n+1} \in \mathbf{H}_0(\operatorname{div}^0; T) \cap \mathbb{P}_n^3$ .

Let us now prove the linear independence of the functions in (20).

Clearly

$$\nabla \times \Psi_{\ell, \alpha}^{n+1} = (n+2) \nabla \times (B_{\alpha-e_{\ell}}^{n+1} \nabla \lambda_{\ell})$$

then, using  $\nabla B_{\alpha}^{n+1} = (n+1) \sum_{k=1}^4 B_{\alpha-e_k}^n \nabla \lambda_k$ , we obtain

$$\frac{1}{(n+1)(n+2)} \nabla \times \Psi_{\ell, \alpha}^{n+1} = \sum_{m=1}^4 B_{\alpha-e_{\ell}-e_m}^n \nabla \lambda_m \times \nabla \lambda_{\ell}.$$

In particular if  $\ell = 1$ , then

$$\begin{aligned} \frac{1}{(n+1)(n+2)} \nabla \times \Psi_{1, \alpha}^{n+1} &= B_{\alpha-e_1-e_2}^n \nabla \lambda_2 \times \nabla \lambda_1 \\ &\quad + B_{\alpha-e_1-e_3}^n \nabla \lambda_3 \times \nabla \lambda_1 \\ &\quad + B_{\alpha-e_1-e_4}^n \nabla \lambda_4 \times \nabla \lambda_1 \end{aligned}$$

and eliminating  $\nabla \lambda_4$  with the aid of the expression

$$\nabla \lambda_1 + \nabla \lambda_2 + \nabla \lambda_3 + \nabla \lambda_4 = \mathbf{0}$$

gives

$$\begin{aligned} \frac{1}{(n+1)(n+2)} \nabla \times \Psi_{1, \alpha}^{n+1} &= (B_{\alpha-e_1-e_4}^n - B_{\alpha-e_1-e_2}^n) \nabla \lambda_1 \times \nabla \lambda_2 \\ &\quad + (B_{\alpha-e_1-e_3}^n - B_{\alpha-e_1-e_4}^n) \nabla \lambda_3 \times \nabla \lambda_1. \end{aligned} \quad (38)$$

Analogous expressions are readily obtained for  $\nabla \times \Psi_{\ell, \alpha}^{n+1}$ ,  $\ell = 2, 3$  by cyclic permutation of the indices 1-2-3.

To simplify notation, we denote the direction vectors

$$\mathbf{t}_{12} := \nabla \lambda_1 \times \nabla \lambda_2, \quad \mathbf{t}_{23} := \nabla \lambda_2 \times \nabla \lambda_3, \quad \mathbf{t}_{31} := \nabla \lambda_3 \times \nabla \lambda_1.$$

It is clear that  $\mathbf{t}_{12}, \mathbf{t}_{23}, \mathbf{t}_{31} \in \mathbb{R}^3$  are linearly independent.



Now, let coefficients  $c_{\alpha}^{(1)}$ ,  $c_{\alpha}^{(2)}$ , and  $c_{\alpha}^{(3)}$  be such that

$$\sum_{\alpha \in \tilde{\mathcal{I}}_3^{n+2}} c_{\alpha}^{(1)} \nabla \times \Psi_{1,\alpha}^{n+1} + \sum_{\alpha \in \tilde{\mathcal{I}}_3^{n+2}} c_{\alpha}^{(2)} \nabla \times \Psi_{2,\alpha}^{n+1} + \sum_{\substack{\alpha \in \tilde{\mathcal{I}}_3^{n+2} \\ \alpha_3=1}} c_{\alpha}^{(3)} \nabla \times \Psi_{3,\alpha}^{n+1} = \mathbf{0}.$$

By (38), we have

$$\begin{aligned} & \left( \sum_{\alpha \in \tilde{\mathcal{I}}_3^{n+2}} c_{\alpha}^{(1)} (B_{\alpha-e_1-e_4}^n - B_{\alpha-e_1-e_2}^n) + \sum_{\alpha \in \tilde{\mathcal{I}}_3^{n+2}} c_{\alpha}^{(2)} (B_{\alpha-e_1-e_2}^n - B_{\alpha-e_2-e_4}^n) \right) \mathbf{t}_{12} \\ & + \left( \sum_{\alpha \in \tilde{\mathcal{I}}_3^{n+2}} c_{\alpha}^{(2)} (B_{\alpha-e_2-e_4}^n - B_{\alpha-e_2-e_3}^n) + \sum_{\substack{\alpha \in \tilde{\mathcal{I}}_3^{n+2} \\ \alpha_3=1}} c_{\alpha}^{(3)} (B_{\alpha-e_2-e_3}^n - B_{\alpha-e_3-e_4}^n) \right) \mathbf{t}_{23} \\ & + \left( \sum_{\alpha \in \tilde{\mathcal{I}}_3^{n+2}} c_{\alpha}^{(1)} (B_{\alpha-e_1-e_3}^n - B_{\alpha-e_1-e_4}^n) + \sum_{\substack{\alpha \in \tilde{\mathcal{I}}_3^{n+2} \\ \alpha_3=1}} c_{\alpha}^{(3)} (B_{\alpha-e_3-e_4}^n - B_{\alpha-e_1-e_3}^n) \right) \mathbf{t}_{31} = \mathbf{0}. \end{aligned}$$

This implies that each term behind the direction vectors  $\mathbf{t}_{12}$ ,  $\mathbf{t}_{23}$ , and  $\mathbf{t}_{31}$  of the above expression is *zero*.

Let us now focus on the term behind  $\mathbf{t}_{31}$ . We have

$$\sum_{\alpha \in \tilde{\mathcal{I}}_3^{n+2}} c_{\alpha}^{(1)} (B_{\alpha-e_1-e_3}^n - B_{\alpha-e_1-e_4}^n) + \sum_{\substack{\alpha \in \tilde{\mathcal{I}}_3^{n+2} \\ \alpha_3=1}} c_{\alpha}^{(3)} (B_{\alpha-e_3-e_4}^n - B_{\alpha-e_1-e_3}^n) = 0 \quad (39)$$

The goal is to show that all the coefficients in the above expression is *zero*. We proceed the proof by mathematical induction on the last index  $\alpha_4$ .

Given  $k \in \mathbb{N}_+$ , if

$$c_{\alpha}^{(3)} = 0 \text{ for } \alpha \in \tilde{\mathcal{I}}_3^{n+2} \text{ such that } \alpha_3 = 1, \alpha_4 \leq k, \quad (40a)$$

$$c_{\alpha}^{(1)} = 0 \text{ for } \alpha \in \tilde{\mathcal{I}}_3^{n+2} \text{ such that } \alpha_4 \leq k, \quad (40b)$$

let us prove

$$c_{\alpha}^{(3)} = 0 \text{ for } \alpha \in \tilde{\mathcal{I}}_3^{n+2} \text{ such that } \alpha_3 = 1, \alpha_4 = k+1, \quad (41a)$$

$$c_{\alpha}^{(1)} = 0 \text{ for } \alpha \in \tilde{\mathcal{I}}_3^{n+2} \text{ such that } \alpha_4 = k+1. \quad (41b)$$

First, by induction hypothesis (40), identity (39) reduces to

$$\sum_{\substack{\alpha \in \tilde{\mathcal{I}}_3^{n+2} \\ \alpha_4 \geq k+1}} c_{\alpha}^{(1)} (B_{\alpha-e_1-e_3}^n - B_{\alpha-e_1-e_4}^n) + \sum_{\substack{\alpha \in \tilde{\mathcal{I}}_3^{n+2} \\ \alpha_3=1, \alpha_4 \geq k+1}} c_{\alpha}^{(3)} (B_{\alpha-e_3-e_4}^n - B_{\alpha-e_1-e_3}^n) = 0 \quad (42)$$

Recursively using  $\lambda_k B_{\alpha}^n = \frac{\alpha_k+1}{n+1} B_{\alpha+e_k}^{n+1}$ , we have

$$B_{\beta}^n = \frac{\binom{n}{k} \lambda_4^k}{\binom{\beta_4}{k}} B_{\beta-k e_4}^{n-k} \text{ for } \beta \in \mathcal{I}_3^n \text{ such that } \beta_4 \geq k.$$

Applying the above identity to (42), and dividing the resulting expression by  $\binom{n}{k}\lambda_4^k$ , we obtain

$$0 = \sum_{\substack{\alpha \in \tilde{\mathcal{I}}_3^{n+2} \\ \alpha_4 \geq k+1}} \left( \frac{c_{\alpha}^{(1)}}{\binom{\alpha_4}{k}} B_{\alpha - e_1 - e_3 - k e_4}^{n-k} - \frac{c_{\alpha}^{(1)}}{\binom{\alpha_4-1}{k}} B_{\alpha - e_1 - (k+1)e_4}^{n-k} \right) \\ + \sum_{\substack{\alpha \in \tilde{\mathcal{I}}_3^{n+2} \\ \alpha_3=1, \alpha_4 \geq k+1}} \left( \frac{c_{\alpha}^{(3)}}{\binom{\alpha_4-1}{k}} B_{\alpha - e_3 - (k+1)e_4}^{n-k} - \frac{c_{\alpha}^{(3)}}{\binom{\alpha_4}{k}} B_{\alpha - e_1 - e_3 - k e_4}^{n-k} \right) \quad (43)$$

Now, evaluating right hand side of (43) on the edge  $E_{34} := F_3 \cap F_4$ , and recalling that  $\lambda_3 = \lambda_4 = 0$  on this edge, we get

$$\sum_{\substack{\alpha \in \tilde{\mathcal{I}}_3^{n+2} \\ \alpha_3=1, \alpha_4=k+1}} c_{\alpha}^{(1)} B_{\alpha - e_3 - (k+1)e_4}^n \Big|_{E_{34}} = 0,$$

which implies the result in (41a) holds true by the linear independence of Bernstein polynomials on the edge. Next, using (41a), evaluating the expression (43) on the face  $F_4$ , and recalling that  $\lambda_4 = 0$  on this face, we get

$$\sum_{\substack{\alpha \in \tilde{\mathcal{I}}_3^{n+2} \\ \alpha_4=k+1}} c_{\alpha}^{(1)} B_{\alpha - e_1 - (k+1)e_4}^{n-k} \Big|_{F_4} = 0$$

which implies the result in (41b) holds true by the linear independence of Bernstein polynomials on the face. This completes the induction proof.

Similar, we can show that  $c_{\alpha}^{(2)} = 0$  for all  $\alpha \in \tilde{\mathcal{I}}_3^{n+2}$ , hence the set (20) form a basis for  $\mathbf{H}_0(\text{div}^0; T) \cap \mathbb{P}_n^3$ , which immediately implies the linear independence of functions in the set (19). This completes the proof of Lemma 2.  $\square$

## REFERENCES

- [1] M. AINSWORTH, *Pyramid algorithms for Bernstein-Bézier finite elements of high, nonuniform order in any dimension*, SIAM J. Sci. Comput., 36 (2014), pp. A543–A569.
- [2] M. AINSWORTH, G. ANDRIAMARO, AND O. DAVYDOV, *Bernstein-Bézier finite elements of arbitrary order and optimal assembly procedures*, SIAM J. Sci. Comput., 33 (2011), pp. 3087–3109.
- [3] ———, *A Bernstein-Bézier basis for arbitrary order Raviart-Thomas finite elements*, Constr. Approx., 41 (2015), pp. 1–22.
- [4] M. AINSWORTH AND J. COYLE, *Hierarchical finite element bases on unstructured tetrahedral meshes*, Internat. J. Numer. Methods Engrg., 58 (2003), pp. 2103–2130.
- [5] D. N. ARNOLD, R. S. FALK, AND R. WINTHER, *Geometric decompositions and local bases for spaces of finite element differential forms*, Comput. Methods Appl. Mech. Engrg., 198 (2009), pp. 1660–1672.
- [6] F. FUENTES, B. KEITH, L. DEMKOWICZ, AND S. NAGARAJ, *Orientation embedded high order shape functions for the exact sequence elements of all shapes*, Comput. Math. Appl., 70 (2015), pp. 353–458.
- [7] R. C. KIRBY, *Low-complexity finite element algorithms for the de Rham complex on simplices*, SIAM J. Sci. Comput., 36 (2014), pp. A846–A868.
- [8] M.-J. LAI AND L. L. SCHUMAKER, *Spline functions on triangulations*, vol. 110 of Encyclopedia of Mathematics and its Applications, Cambridge University Press, Cambridge, 2007.
- [9] C. LEHRENFELD, *Hybrid Discontinuous Galerkin methods for solving incompressible flow problems*, 2010. Diploma Thesis, MathCCES/IGPM, RWTH Aachen.

- [10] C. LEHRENFELD AND J. SCHÖBERL, *High order exactly divergence-free hybrid discontinuous galerkin methods for unsteady incompressible flows*, Computer Methods in Applied Mechanics and Engineering, 307 (2016), pp. 339–361.
- [11] J.-C. NÉDÉLEC, *Mixed finite elements in  $\mathbf{R}^3$* , Numer. Math., 35 (1980), pp. 315–341.
- [12] S. ZAGLMAYR, *High order finite element methods for electromagnetic field computation*, 2006. PhD thesis, Johannes Kepler Universit ät Linz, Linz.

DIVISION OF APPLIED MATHEMATICS, BROWN UNIVERSITY, 182 GEORGE ST, PROVIDENCE RI 02912, USA.

*E-mail address:* `Mark_Ainsworth@brown.edu`

DIVISION OF APPLIED MATHEMATICS, BROWN UNIVERSITY, 182 GEORGE ST, PROVIDENCE RI 02912, USA.

*E-mail address:* `Guosheng_Fu@brown.edu`